GEOLOGY OF THE MCMILLAN RANCH IN MASON, TEXAS; AN ASSESSMENT OF THE NATURE OF NORMAL FAULTS IN THE MASON AREA

A Thesis

by

REBECCA ANNE HARPER

Submitted to the Office of Graduate Studies of
Texas A&M University
in partial fulfillment of the requirements for the degree of

MASTER OF SCIENCE

August 2011

Major Subject: Geology

Geology of the McMillan Ranch in Mason, Texas; An Assessment of the Nature of Normal Faults in the Mason Area

GEOLOGY OF THE MCMILLAN RANCH IN MASON, TEXAS; AN ASSESSMENT OF THE NATURE OF NORMAL FAULTS IN THE MASON AREA

A Thesis

by

REBECCA ANNE HARPER

Submitted to the Office of Graduate Studies of
Texas A&M University
in partial fulfillment of the requirements for the degree of

MASTER OF SCIENCE

Approved by:

Chair of Committee,	Christopher C. Mathewson
Committee Members,	John R. Giardino
	James B. Kracht
	Michael J. Heaney III
Head of Department,	Andreas Kronenberg

August 2011

Major Subject: Geology

ABSTRACT

Geology of the McMillan Ranch in Mason, Texas: An Assessment of the Nature of Normal Faults in the Mason Area. August 2011

Rebecca Anne Harper, B.S., Texas A&M University

Chair of Advisory Committee: Dr. Christopher C. Mathewson

Mason, Texas and the surrounding areas have been previously studied and mapped at small scales, showing the large normal faults that cut through the area. Many secondary faults exist close to the large faults, and are not mapped in previous studies because of the small scale of the maps. The large number of faults, when the smaller secondary faults are considered, makes Mason a good place for studying the nature of normal faults in this region and making generalizations about their nature. This thesis examines one of these faults, the McMillan Fault, and the secondary faults in its hanging wall at a large scale, in order to assess the nature of normal faults in the Mason area.

The McMillan Ranch in Mason, Texas, was mapped at a scale of 1:7,000 using both traditional and digital mapping methods, to determine the lengths and displacements of each fault, and attempt to determine a length/displacement ratio which can be applied to all normal faults in this area. A single length/displacement ratio was not determined, just as in previous studies. This study determined that the normal faults in the area are planar, high angle normal faults with varying displacement amounts. As a

result, observations determined that deformation in the hanging wall of normal faults exceeded the deformation in the footwalls of the same faults. The main fault on the McMillan Ranch is the McMillan Fault, and its shape is determined based upon the orientation of the subsidiary normal faults in its hanging wall.

A detailed study of the geology of the McMillan Ranch and the surrounding area, including a geologic history of the area, geologic map and cross section, and stratigraphic descriptions including bed-by-bed descriptions, stratigraphic column, and thin sections of each unit was carried out as a preliminary step to perform analyses of the faults on the ranch. The presence of the McMillan Fault was already known, and the pasture that was chosen for this study was best represented at a scale of 1:7,000. At such a large scale, it was necessary to recognize precisely where in the stratigraphic section the mapper was located, as some subsidiary faults were recognized by beds missing, rather than entire units.

The structural data gathered from the field convey the varying natures of faults, even within the same area, and support the conclusion that length alone is not sufficient to predict displacement value on a fault.

DEDICATION

Dedicated with love to my father, Dr. Arthur L. Harper ’74, who was the first person to show me how much fun it is to go out and look for rocks.

ACKNOWLEDGEMENTS

First and foremost, I thank my committee chairman, Dr. Christopher C. Mathewson, for taking me as a graduate student and providing guidance and advice in this project, and for being patient with me as I completed it.

Thank you also to Dr. John R. “Rick” Giardino and Dr. Jim Kracht for their many hours of reviewing, editing, and advising. And, also, for your never-ending patience with me!

This thesis could not have been completed without the help of Dr. Michael J. Heaney III. Thank you for the many days, weekends, and spring breaks spent in Mason, Texas, helping me with the mapping and other areas of field work. I truly appreciate what you taught me about field work, paleontology, the genius of Jerry Garcia, and making a mean eggplant ratatouille!

Thank you to Mrs. Tammy Gardner at the Hill Country Inn in Mason, Texas, and also to the Mason Mountain Wildlife Management Area for providing lodging to our many visits to Mason.

I am very grateful to Mr. and Mrs. Hal McMillan and Mr. Kolin Kothmann for providing access to their properties and being so helpful throughout this work. Thank you so much for letting us invade your ranches every week!

And finally, thank you, Mom, for watching the dogs every weekend I was gone! I couldn’t have done it without your help.

TABLE OF CONTENTS

LIST OF FIGURES

FIGURE Page

FIGURE Page

LIST OF TABLES

CHAPTER I

INTRODUCTION:

REGIONAL SETTING AND GEOLOGIC HISTORY

The city of Mason is located in Mason County, Texas, which is located in the western portion of the Llano Uplift (Figure 1). Numerous large normal faults are present throughout the area. The Llano Uplift was formed through multiple, repeated series of uplift and subsidence from the Precambrian to the Miocene (Becker, 1985). Extensive normal faulting was likely a result of the Ouachita Orogeny, which was marked by the collision of the North American and African plates. It is hypothesized that during collision, the edge of the subducting plate can become so loaded with sediment accumulation and the weight of the overriding plate that it bends, putting extensional strain on the upper portion and creating a series of normal faults (Becker, 1985). The regional strike of the bedding in the area is generally northeast and beds generally dip slightly to the southeast.

The geology in Mason County ranges from Precambrian granite and schist to Pennsylvanian limestone. The study area contains eight different sandstone and limestone units with a smaller range of ages: lower Cambrian to Ordovician in age.

The study area is located on the McMillan Ranch (Figure 1), which ranges from

---

This thesis follows the style of Geology.

an elevation of 518-536 m. Mean annual precipitation in the area is 66 cm, and the mean annual temperature is ~18.8º C (Singhurst et al. 2007).

Vegetation types occur in association with one another and correspond to the underlying geology (Singhurst et al., 2007). Common on the McMillan Ranch are the Roundleaf, Catclaw-Texas, Yucca/Texas, Pricklypear-Agarito association, which occurs on the Hickory Sandstone Formation. Ferns exist near northeast-facing hanging rock shelves, as well as perennial grasses and small shrubs. Also common is the Mesquite-Whitebrush-Texas, Pricklypear-Texas Persimmon Association (Singhurst et al., 2007).

The McMillan Ranch is located west of the city of Mason and is used for cattle ranching, whitetail deer hunting, and horse pastures. The fenced pastures used for hunting and the pastures used for horses are determined in part by the underlying

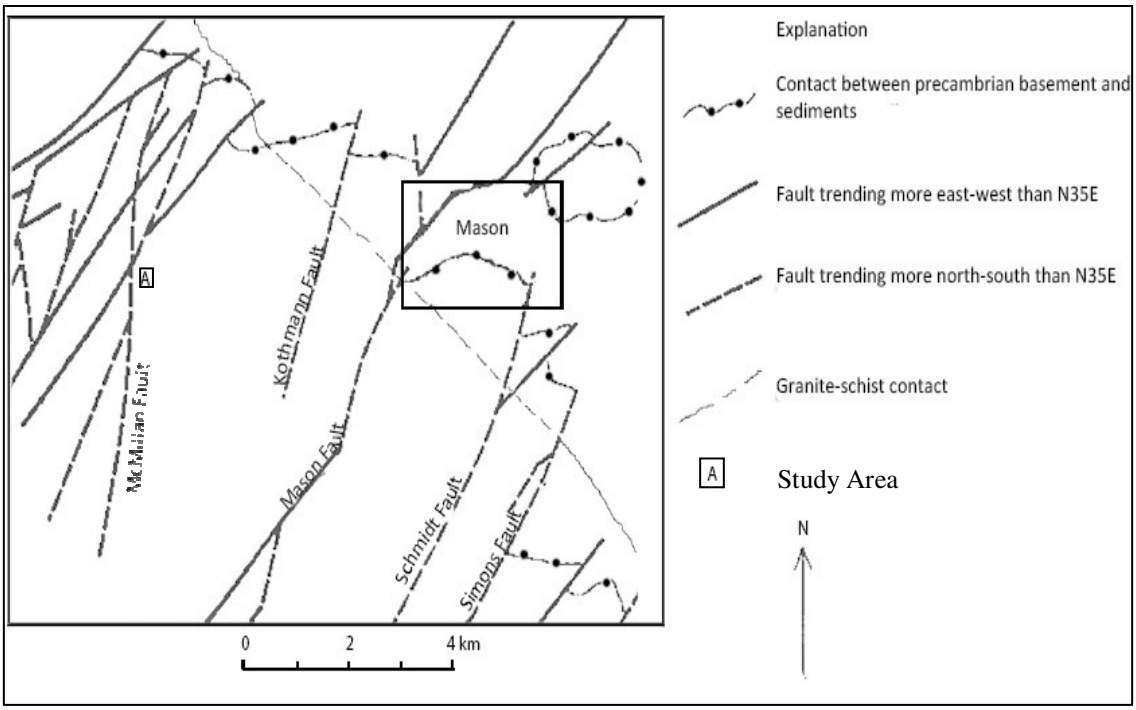

Figure 1. Location of Mason, Texas, and of the study area (Enlarged portion adapted from Becker, 1985).

geology. Pastures underlain by the Hickory sandstone produce fields of grasses suitable for horses, whereas the pastures underlain with combinations of many limestones and sandstones produce various vegetation types, suitable for deer habitats.

The ranch is located just off of FM 1788 outside of Mason. To access the ranch one travels west out of Mason on state Hwy 87 to Hwy 377. FM 1788 turns southwest off of Hwy 377. Permission to access to the study area was granted by Mr. and Mrs. Hal McMillan.

Deformation Structures in the Mason Area

Fracture sets in the Mason area are categorized into three different types: 1) straight, planar fractures of a single orientation, 2) segmented fractures consisting of joined segments of two or more orientations, and 3) en echelon fractures. Segmented fractures are the most common and en echelon fractures are the least common (Becker, 1985).

Usually, individual fractures cannot be traced for more than a few meters, because the exposure of the outcrops is limited. Fracture widths vary. Width can be affected by the amount of dissolution weathering along the fractures, which is dependent, in part, on lithology. Most fractures are open, but occasional filled fractures occur. In limestones and dolomites, the fill material tends to be calcite (Becker, 1985). More than one fracture set usually occurs at an outcrop, one set being dominant. If two or three different sets occur in approximately equal proportions, a rhomboidal pattern occurs. The abundance of fractures varies by lithology, with the dolomites having the highest fracture frequencies and sandstones having the lowest (Becker, 1985).

Breccias may also be related to faulting, though not always. In the Mason area, breccias have three structural associations: 1) they may be related to faults; 2) they may occur as layers parallel to bedding; or 3) may be found in diffuse zones, not clearly associated with well defined faults (Becker, 1985). In the Mason area, the most common breccias are associated with faults (Becker, 1985). Breccia zones along major faults typically are one to twenty meters wide, usually depending on the lithologies of the hanging wall and footwall. Minor faults either lack breccia zones or have zones less than half-a-meter wide.

Characteristics of the Mason Area Faults

The major faults of the Mason area generally trend to the northeast, unless a change in basement lithology occurs. In this case, the faults trend more to the north (Barnes, 1981; Becker, 1985). The basement rock consists of the Town Mountain Granite and the Packsaddle Schist, with the contact between the two trending to the northwest. Maximum throws on the major faults of the area tend to increase as they approach the Packsaddle Schist and tend to show more branching and splaying (Becker, 1985).

Geologic History of the Llano Uplift

Grenville Orogeny

The Llano Uplift was formed during the Grenville orogenic event ca. 1150-1120 Ma. It is one of several orogenic belts associated with Grenvillian time. These belts are the result of a collision between a continent off the southern Laurentian boundary as Rodinia formed (Mosher, 1998).

The eastern margin of Laurentia was bordered by the Grenville orogen. Orogenesis occurred both as a result of collisions of separate bodies and intracratonic (within the North American craton) processes (Mosher, 1998). Some plate reconstructions indicate that South America was the continent that collided with North America to form this orogen (Dalziel, 1991, 1992, 1997; Hoffman, 1991; Moores, 1991; Unrug, 1996) whereas others show western Africa as the colliding continent (Bird and Dewey, 1970; Hatcher, 1987, and others).

The Llano Uplift in central Texas represents an orogen on the southern side of Laurentia. Geologic studies of the area suggest both a continent-continent collisional orogenesis and arc-continent orogenesis (Carlson, 1998; Wilderson, et al., 1988; Mosher, 1993; Mosher, 1998; Reese, 1995; Roback, 1996a). The Llano Uplift located approximately 300 km south of the northeast-trending Llano front. The Llano front is a magnetic and gravity anomaly that is similar to the Grenville front in the Appalachians of the eastern United States (Mosher, 1993 and 1998). The Llano Uplift exposes the core of the southern Grenville orogen and shows a suture between an arc terrane and continental crust (Roback, 1996; Mosher, 1998). Other exposures near Van Horn, Texas, expose the northern margin of the orogen, which is believed to be a continuation of the Llano front (Mosher, 1998).

Emplacement of Basement Rock

The rocks of the Llano Uplift are ca. 1360-1232 $\pm$ 4 Ma. They consist of metavolcanic, metaplutonic, and metasedimentary rocks that have undergone low to medium pressure regional metamorphism (upper amphibolite to lower granulite facies)

(Mosher, 1998; Mosher, 2008). These sedimentary rocks were then intruded by granites of ages 1119-1070 Ma.

Three lithologic domains make up the Precambrian stratigraphy of the Llano Uplift (Mosher, 1996; Roback, 1996; Mosher, 1998; Mosher, 2008). The southernmost of these is the Coal Creek domain, which is a tonalitic to dioritic arc terrance (Garrison, 1981b, 1985; Roback, 1996a). The Coal Creek structurally overlies the Packsaddle domain, which consists of metavolcanic and metasedimentary supracrustal rocks intruded by metaplutonic rocks and is interpreted as a forearc basin (Mosher, 1998; Smith, et al., 2010). The Packsaddle domain structurally overlies the northernmost Valley Spring domain, a granitic gneiss terrane. The Valley Spring domain has supracrustal and plutonic rocks, as well as an older crustal component (ca. 1360 Ma) that may represent the southern margin of Laurentia (Reese et al., 1992; Reese, 1995; Roback, 1996a; Mosher, 1998). Each of these domains were deformed, thickened, and metamorphosed to middle amphibolite facies during the Grenville orogeny (Nelis, 1989).

Emplacement of Igneous Intrusions

The metamorphic rocks of the Llano Uplift were intruded by tectonic granites 1119-1070 Ma (Smith, et al., 2010). These groups of granites are collectively called the Town Mountain Granite. The Town Mountain Granites have been divided into two groups based on intrusion shape and internal fabric (Reed, 1996a and Smith, et al., 2010). One group has elongate to irregular-shaped plutons with solid-state deformation, including the Wolf Mountain, Legion Creek, and Grape Creek plutons (Smith, et al.,

2010), and the other group typically has undeformed circular to oval-shaped plutons, including the Lone Grove, Kingsland, Marble Falls, Enchanted Rock, and Katemcy plutons (Smith, et al., 2010).

Paleozoic

Sedimentary rocks in the Llano Uplift rest unconformably upon the Precambrian igneous and metamorphic rocks described previously. The sedimentary rocks in the Mason area are of Cambrian and early Ordovician age and belong to the Riley and Wilberns Formations. The Cambrian rocks represent both terrestrial and marine environments that covered the area at different periods of time (Chafetz, 1980).

The lower Riley Formation shows evidence of a transgressive-regressive sequence. The Riley Formation is shown by the basal Hickory sandstone overlain by the Cap Mountain limestone followed by the Lion Mountain sandstone. The Hickory Sandstone is composed of six lithofacies which were deposited within a "non barred tidally-influenced or estuarine-related" environment (Cornish, 1975a; Chafetz, 1980). Occasional fining-upward sequences in the Hickory Sandstone indicate tidal and tidal channel deposits. These interfinger with shallow shelf carbonates (Cornish, 1975a; King, 1976; Chafetz, 1980). These shelf carbonates were deposited across much of the area, and oolite shoals developed on the platform margin (Chafetz, 1980). These ooids are visible in the upper Hickory sandstone, just below the onset of the Cap Mountain limestone.

The Wilberns Formation shows a similar transgressive-regressive sequence, deposited over a disconformity surface. The Wilberns contains the basal Welge

sandstone, overlain by the Morgan Creek limestone, followed by the Point Peak siltstone, then the San Saba carbonates. The basal Welge and overlying carbonates seem to have accumulated in an intertidal to turbulent, shallow marine environment, with water depths probably never exceeding 5-10 m (Chafetz, 1980). Turbulence and water depth decreased with increasing height in section (Chafetz, 1980). As one progresses upsection into the San Saba carbonates, there is a return to shelf carbonate accumulation (Chafetz, 1980).

According to the literature, there are no terrestrial deposits within the section.

Ouachita Orogeny

During the middle Pennsylvanian, the supercontinents of Gondwana and Laurentia collided, inducing the Ouachita mountain-building event (Sloan, 1998). This orogenic event can be traced from Texas, northeast into the Appalachian Mountains. It is believed that as the North American plate collided with the African plate, sediment accumulated on the North American plate. This loading led to plate flexure parallel to the convergent zone to the southeast, resulting in extension in the upper portion of the plate (Becker, 1985). The normal faults found in the Mason area are a result of this flexure. Most of these faults trend northeast-southwest, which parallels the Ouachita orogeny, offering further evidence of the relationship between the two (Becker, 1985).

Post-Ouachita History

The rocks of the Llano Uplift which outcrop presently are a result of the intersection of several arches (Figure 2), which intersect at the Llano Uplift (Ewing, 2005).

The Concho Arch stretches from the Texas panhandle to Llano along a broad northwest-southwest trending axis. This area once received thick Cambrian and lower Ordovician sediments, but the arch thinned the strata along its axis.

The Bend Arch formed during the Pennsylvanian along the western edge of the Fort Worth foredeep basin and the eastern margin of the late Pennsylvanian to Permian West Texas Basin (Ewing, 2005). The Llano Uplift is at the southern end of this Arch. It is believed that the early Pennsylvanian normal and transtensional faulting (Llano Fault Zone) was related to the foredeep development (Ewing, 2005).

The Llano Uplift is at the eastern edge of the late Pennsylvanian to Permian Ozona Arch. This arch is a forebulge arch, which is related to the Val Verde Basin to the south (Ewing, 2005).

As the Gulf of Mexico opened in the middle Jurassic, a northeast trending rift shoulder formed. The Llano Arch formed along this rift shoulder, uplifting and eroding Paleozoic sediments. The Llano Arch shows the junction of previous arches (Ewing, 2005).

The final arch to affect the Llano Uplift is the San Marcos arch, which formed a southeast-trending forebulge to the Maverick Basin during middle and late Cretaceous.

In the Neogene, the entire North American Cordillera experienced uplift, thus uplifting the Llano area once more. During this time, differential subsidence and slippage created the Balcones Fault Zone along Ouachita lines of weakness (Ewing, 2005).

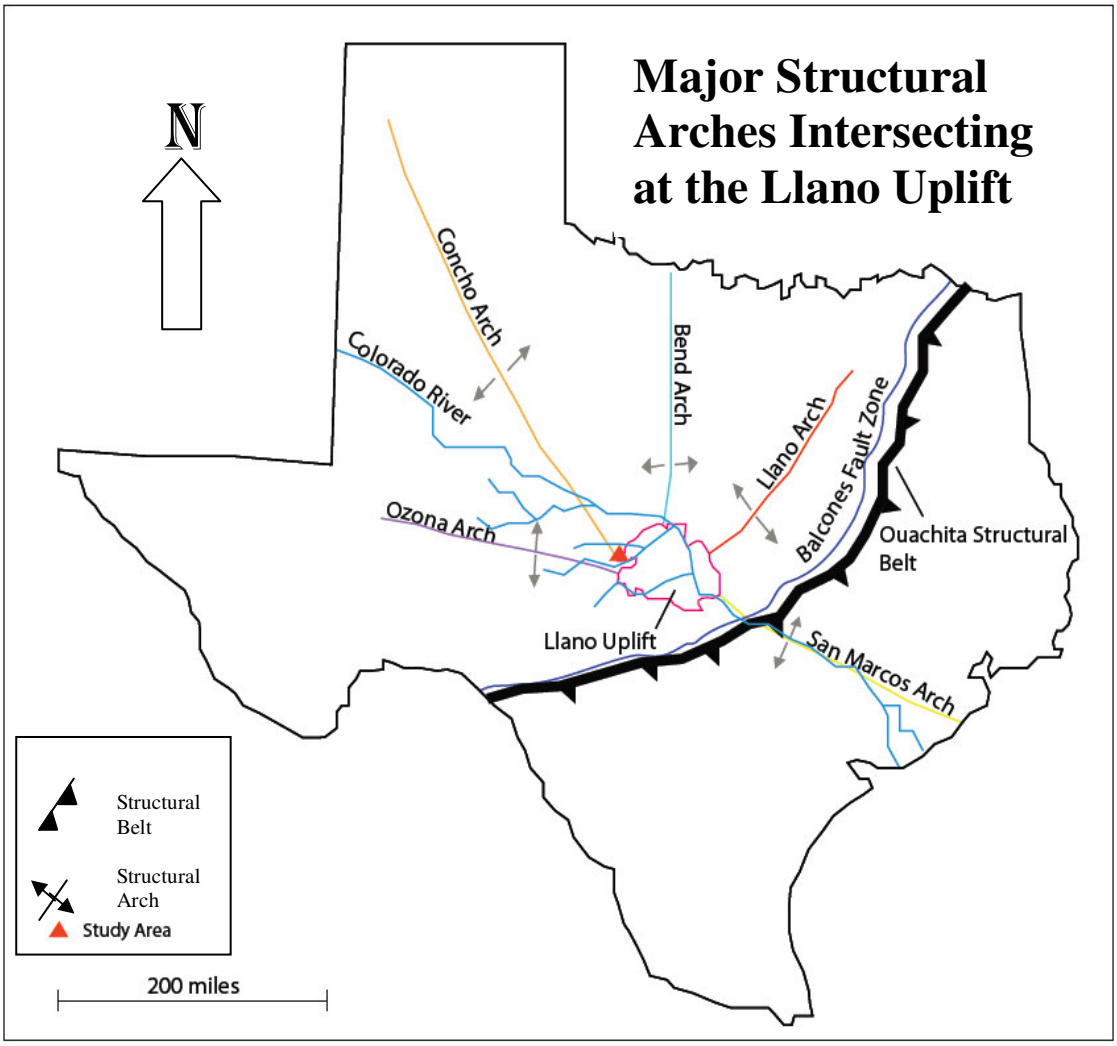

Figure 2. Schematic map of Texas showing the location of the Llano Uplift as it is related to major structural arches, the Colorado River, and the Ouachita Structural Belt, all of which led to the Precambrian rocks of the Llano Uplift being exposed today. (Adapted from works by Ewing, 2006; Wermond, 1996;Nelis, et al., 1989).

In addition to this structural uplift of the region, the Llano area was subjected to erosion as a result of glacial events. During each glacial event Texas climate was cooler and wetter. This increased both chemical and physical weathering with increased erosion. Additionally, as the glaciers melted, the massive flow of water through the Colorado and Llano rivers caused erosion to occur in the Llano region, further removing sedimentary layers and exposing the Precambrian core. The increased flow in the rivers also accounts for dramatic river terraces on either side of the modern-day Colorado River near Austin, and for the transport of large granite boulders great distances downstream.

CHAPTER II

METHODOLOGY

As preliminary reconnaissance work, geologic maps were created on mylar sheets overlain on aerial photographs of the McMillan Ranch, at a scale of 1:7,000. These maps were created by walking the contacts and faults and drawing their positions directly onto the overlay. Strike and dip data and other important observations were noted at this time**.** These traditional mapping methods allowed the mapper to record an overview of what was seen using a method that was familiar to her, while learning to use the Tablet computers.

Using the traditionally created maps as guides, an Xplore® iX104C3 Tablet andBluetooth® Global Positioning System (GPS) receiver were used to create a more accurate, digital geologic map. A digital orthophotograph of the area was uploaded into ArcMap® in the laboratory, and layers for contacts, faults, units, and outcrops were created. This information was saved to the Tablet and used in ArcPad® while in the field to create a digital geologic map. Well-constrained contacts were followed on foot, with the GPS on tracking mode. This tracklog was then used to draw the contact on the Tablet. For other, less well-constrained contacts, waypoints were taken on outcrops, and a contact inferred between them. Each unit was assigned a different symbol as its waypoint, to aid in inferring contacts between them.

The traditional and digital maps were the basis for all following structural analyses, including the creation of the cross section, determining fault length-displacement ratios, and determining the relationships between the faults and hanging-

wall deformation. Most of these relationships were determined geometrically, by actually drawing the faults and using trigonometry to determine the dip slip, throw, and heave. The traditional mapping methods were simpler to use to gain an overview of the faults on the ranch. When the time came to finalize the more intricate details of the map, digital mapping methods allowed the faults to be more precisely located. This was especially useful in portions of the ranch that were far from roads or other landmarks, which were used to locate features on the traditional map. The GPS receivers were accurate to within a few meters and proved very helpful. Traditional mapping techniques allowed accuracy to within a meter in cases where landmarks made determining location on the aerial photograph easy. Determining location was only reliable, however, on the margins of the mapping area where roads were located. Within the ranch, dense vegetation made determining locations difficult. The GPS receivers also needed to be charged, however, and occasionally did not connect to the Tablet, so it was necessary to have several charged and on hand, in case one lost its signal.

CHAPTER III

STRATIGRAPHY

The oldest sedimentary unit in Mason is the Cambrian-aged Hickory sandstone, which is divided into a lower, middle, and upper member. These are well-exposed inroadcuts along FM 2618, just to the east of Mason. The Hickory sandstone is part of the Riley formation.

All three members of the Hickory are quartzose sandstones. The lower member is cream-colored to light brown when fresh and weathers to a darker brown and black. The lower member may be considered bimodal. Grain sizes vary from fine to very coarse (Figure 3). The grains tend to be subrounded and poorly sorted. The unit is poorly cemented, held together by "dissolution cement", cement formed by the dissolution and reprecipitation of minerals, exhibits massive bedding, and weathers to slopes.

The middle member of the Hickory sandstone is orange when fresh and weathers to lighter orange, tan, and/or black. Like the lower member, the middle Hickory has grains which range from fine to very coarse, are subrounded, and are poorly sorted. Porosity ranges from medium to low. This member is moderately well to well cemented with hematite cement. Beds tend to range from thin to thick (Figure 4). This member weathers to slopes, and may show trace fossils (rusophycus, Figures 5 and 6).

Figure 3. Closeup of grains of the Hickory sandstone. Note cross-stratification in the upper portion of photograph (circled). Note hammer for scale.

Figure 4. Beds of middle Hickory sandstone. Note human for scale.

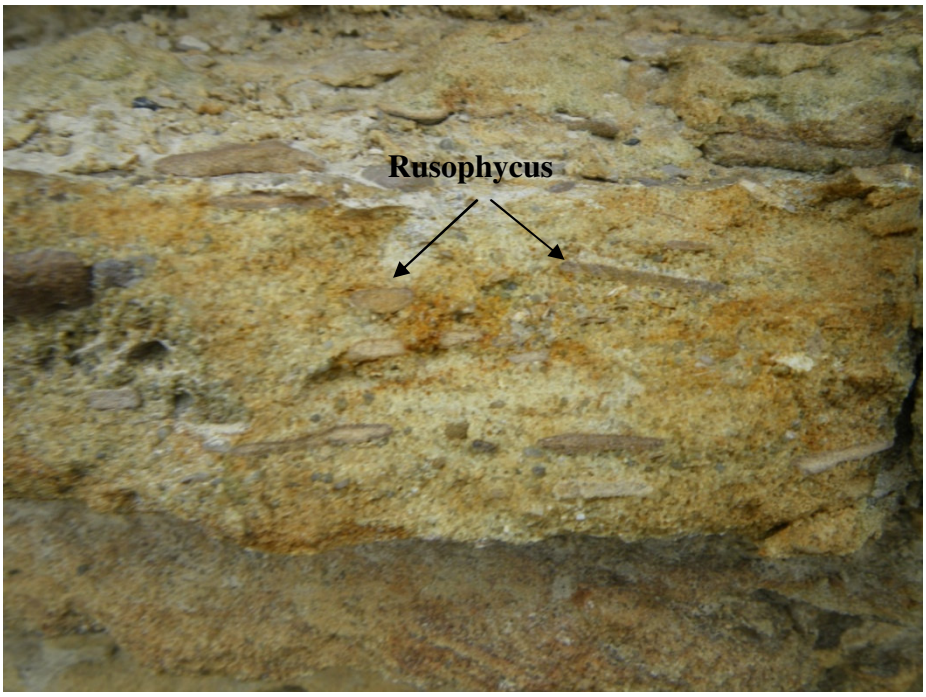

Figure 5. Rusophycus in the middle Hickory sandstone (linear features), viewed from the side of a bed.

Figure 6. Rusophycus in the middle Hickory sandstone (circled), viewed from the bottom of a bed. Note thumb for scale.

The upper member of the Hickory sandstone is a reddish-brown sandstone that weathers to orange and brown. The grains are poorly sorted, fine to medium in size (.25-1mm), and subangular. The upper Hickory is often very well cemented with hematite cement, though thedegree of cementation is variable. The upper member is moderately porous. This member may contain dark veins and visible laminations. Iron nodules and inarticulate brachiopods may also be present, as well as characteristic hematite ooids (Figure 7). The upper member of the Hickory sandstone and all younger units to be discussed outcrop in stratigraphic order on the Kothmann Ranch off of Koocksville Road in Mason. Thin sections of the Hickory sandstone are shown in Figures 8 and 9. Above the Hickory sandstone is the Cap Mountain limestone, also of the Cambrian-aged Riley formation. This unit is divided into a lower and upper member.

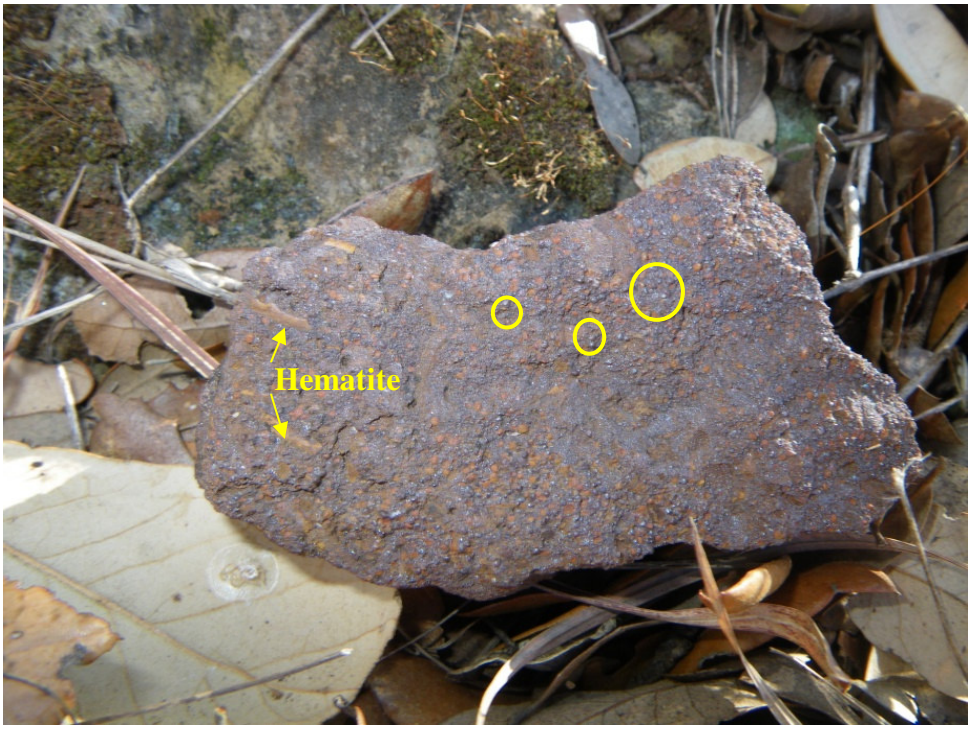

Figure 7. Upper Hickory sandstone, showing hematite ooids (some are circled) and cement.

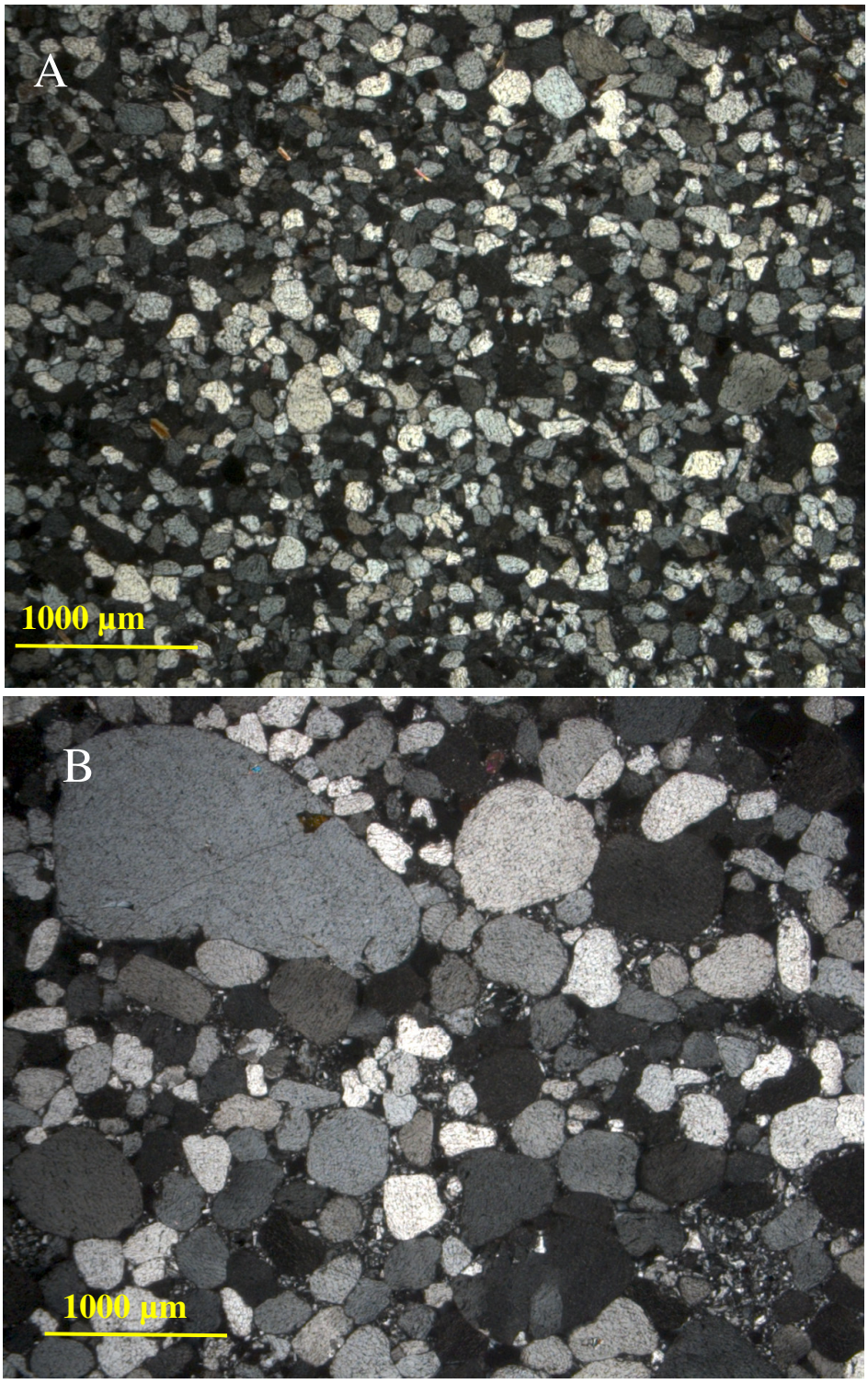

Figure 8. Thin Sections of the lower (A) and middle (B) Hickory sandstone. Note poor sorting in each.

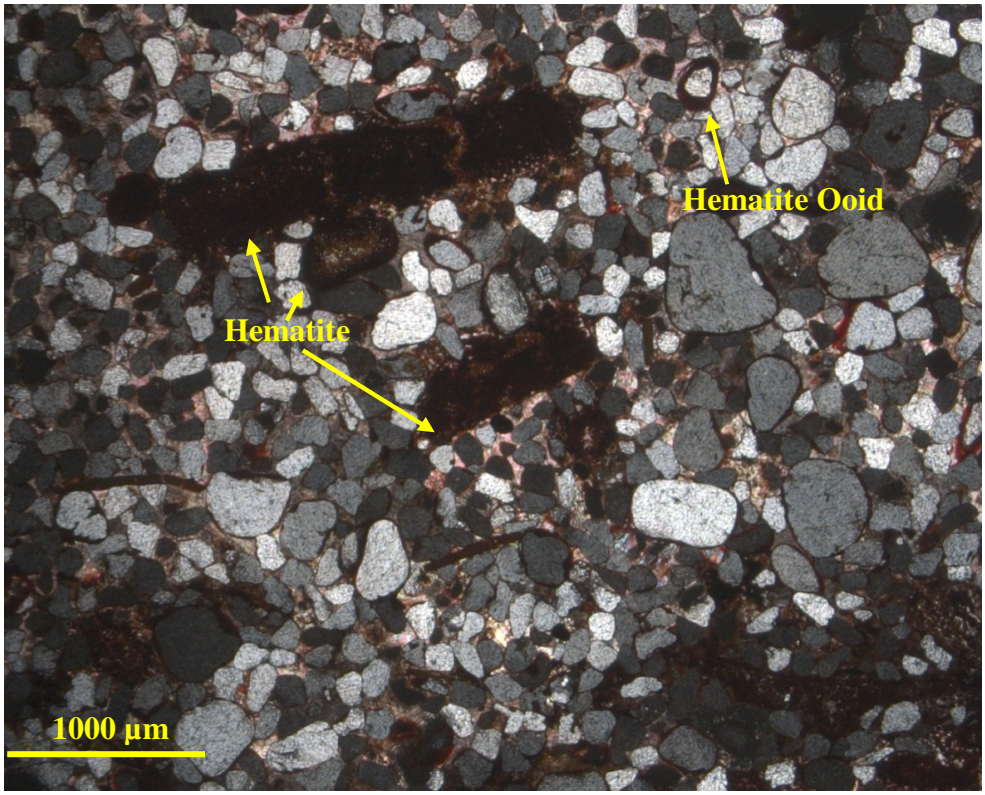

Figure 9. Thin section of the upper Hickory sandstone. Notice the hematite cement (red) and hematite ooids.

The lower Cap Mountain is a quartz-arenite, that is maroon when fresh and weathers to a light-dark red. Striking it with a hammer will produce white streaks. The grains are fine to coarse, subrounded, and moderately well to well sorted. This member is highly quartzose, moderately porous, and well-cemented. It forms slopes, and may be fossiliferous.

The upper member of the Cap Mountain is a calc-arenite. When fresh, colors range from white to gray to brown, and it weathers to a darker grey and/or brown. The unit is fine to very coarse grained, and the grains tend to be subrounded and poorly sorted. The upper member contains more obvious amounts of calcite and glauconite (Figure 10). The upper member is well cemented with calcite cement and non-porous, tends to be thickly bedded to massively bedded, and weathers to “ledgy slopes”. This member may also be fossiliferous.

The remainder of the units are described based upon outcrops at the Kothmann Ranch in Mason, Texas. There, the units outcrop in stratigraphic order without disturbance. The McMillan Ranch contains too many faults for this to be possible there.

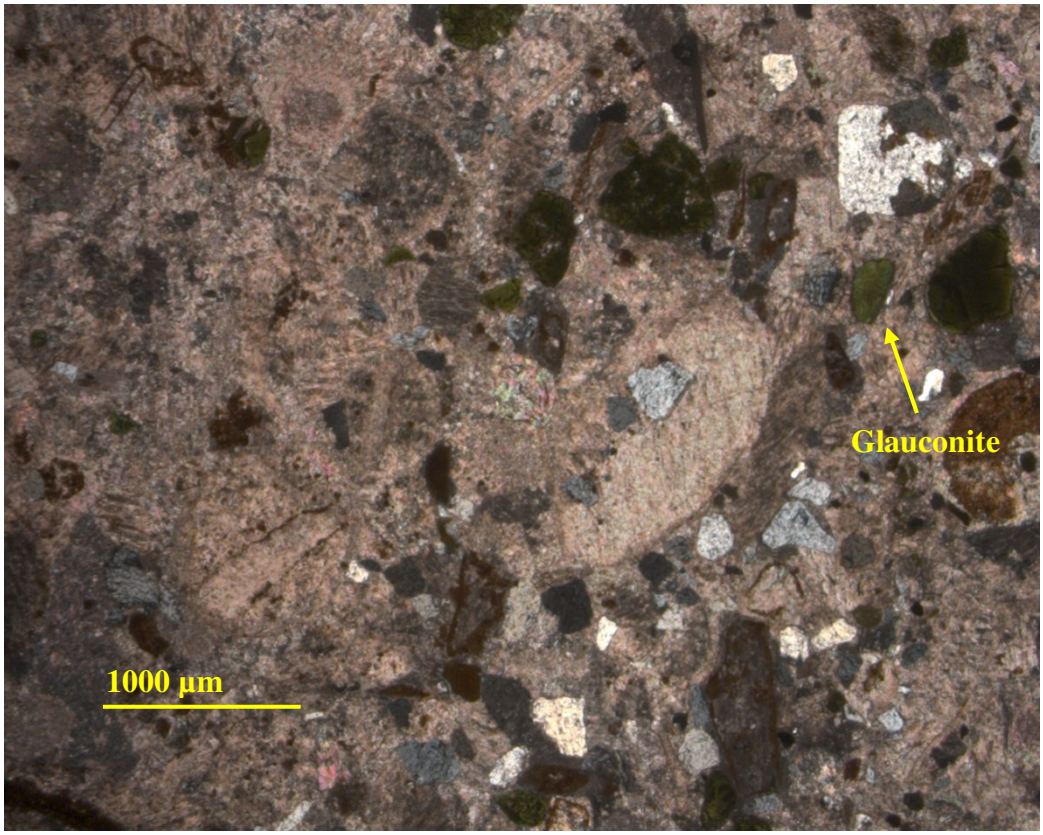

Figure 10. Thin section of the Cap Mountain Limestone, showing abundant calcite cement and sparse glauconite. This thin section is shown in natural light.

The unit above the Cap Mountain is the Lion Mountain, of the Riley formation. In the Mason area, this unit is composed of two distinct lithologies that are found intermixed. In other areas of Texas, these lithologies are often separated into distinct beds. One lithology found in the Lion Mountain is a calc-rudite. When fresh, it varies from grey, white, brown, or green and weathers to grey. Grains are fine to very coarse, subangular, and moderately well cemented with calcite cement and hematite cement. It forms slopes but forms occasional ledges within the slopes, and contains a highly visible, distinct trilobite hash on and inside the bed (Figure 11). The other lithology is a bright green, coarse-grained, well rounded and sorted glauconitic sandstone.

Above the Lion Mountain is the Welge sandstone (Figure 12). The Welge is light to dark orange when fresh and weathered. It is very fine grained to coarse grained. Grains are subrounded and poorly sorted. This unit is quartzose, hematitic, and moderately porous. It is very friable, and the degree of cementation ranges from poor to medium. The Welge weathers to slopes and is fossiliferous.

The next unit, moving up the stratigraphic section is the Morgan Creek limestone, which is divided into lower and upper members.The lower Morgan Creek is a quartz arenite which is white or rust-colored when fresh and weathers to brown.

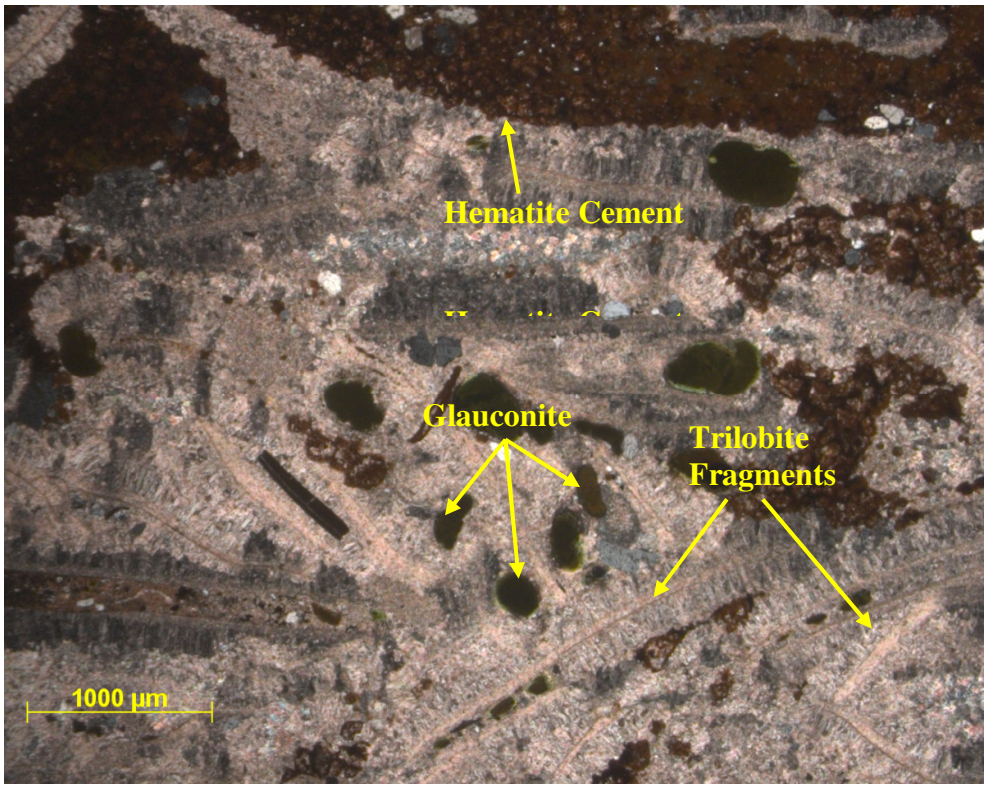

Figure 11. Thin section of the Lion Mountain limestone. Note abundant glauconite, hematite cement, and trilobite fragments.

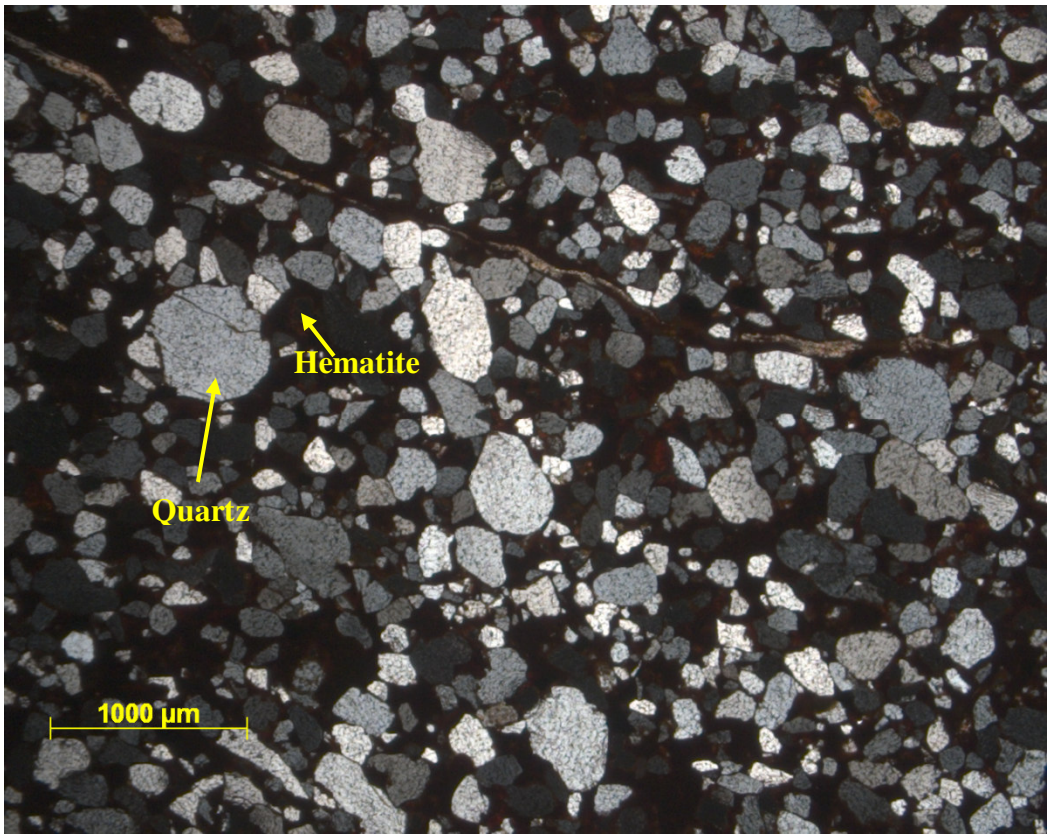

Figure 12. Thin section of the Welge sandstone. This thin section is in natural light, and quartz grains are well-defined because of the presence of hematite.

The next unit, moving up the stratigraphic section is the Morgan Creek limestone, which is divided into lower and upper members.The lower Morgan Creek is a quartz arenite which is white or rust-colored when fresh and weathers to brown. Grains are medium to very coarse, subrounded, and poorly to moderately sorted. This member is quartzose, shows low porosity and is well-cemented with calcite cement. The Morgan Creek forms ledges.The upper Morgan Creek is a calcarenite, and is white and light pink when fresh and weathers to grey. The grains are fine to medium, subrounded, and moderately sorted. This member is calcareous and shows low porosity and is well cemented with calcite cement. It forms ledges. This member is glauconitic and/or fossiliferous, depending upon the sample (Figure 13).

Above the Morgan Creek is the Point Peak limestone, which is divided into lower, middle, and upper members.

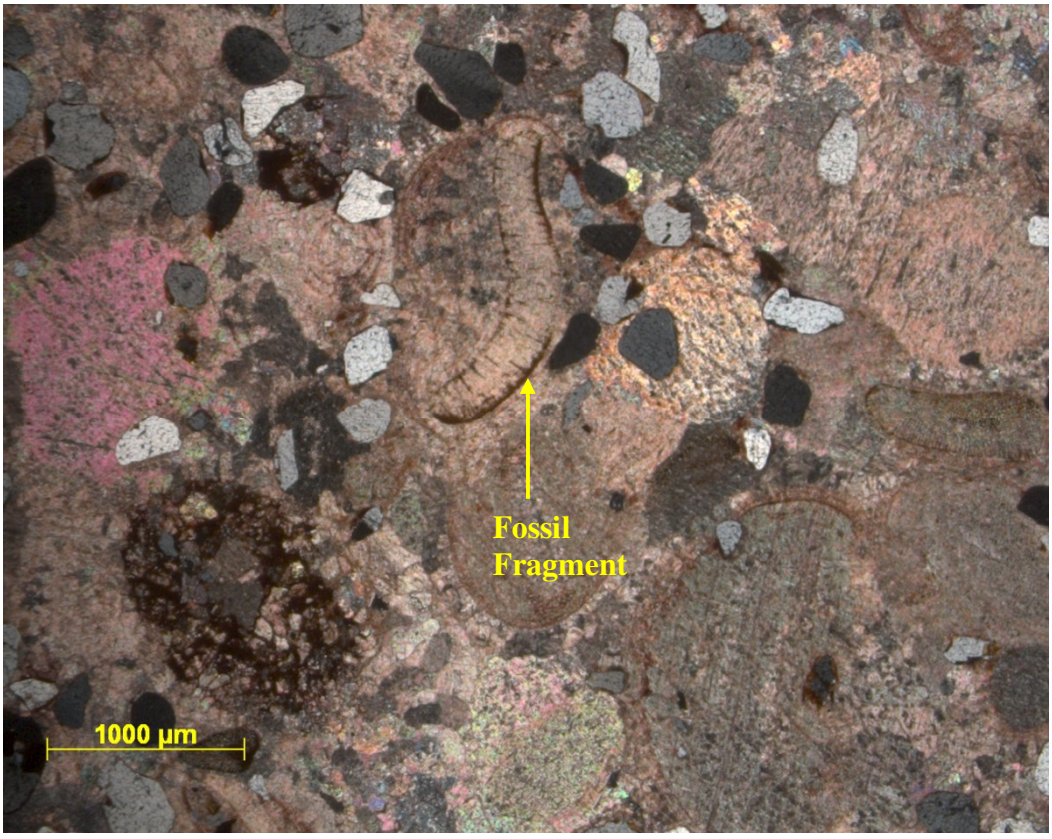

Figure 13.Thin section of the Morgan Creek limestone, showing calcite cement and an unidentified fossil fragment.

The lower Point Peak is a calcisiltite. When fresh it is green-grey and weathers to brown-grey. Grains are very fine, subrounded, and well sorted (Figure 14). This unit is calcareous, shows low porosity, and is well cemented with calcite. The lower Point Peak is thickly bedded and forms slopes. Micrite inclusions are common. Occasionally, one may find fine-grained purple beds. In the lower Point Peak flat pebble conglomerates and sparse glauconite also exist.

The middle Point Peak member is a truer mudstone, lacking inclusions. When fresh it appears orange-brown, almost peach at times and weathers to buff-black. The unit is very fine-grained, well sorted, and calcareous. Porosity is low and the degree of cementation is high with calcite cement. This member is also thickly bedded and weathers to ledges (Figure 15). A distinct pattern of curls appears on top of these beds. Bioherms can be found, and stromatolites are characteristic (Figure 16). A thin section of the middle point peak is shown in Figure 17.

Figure 14. Thin section of the lower Point Peak limestone, a calcsiltite. Notice microscopic layering of grains (some emphasized by dashed lines).

Figure 15. Ledges of Point Peak limestone, shown adjacent to a creek (A) and on a slope (B). Note trees, cacti for scale.

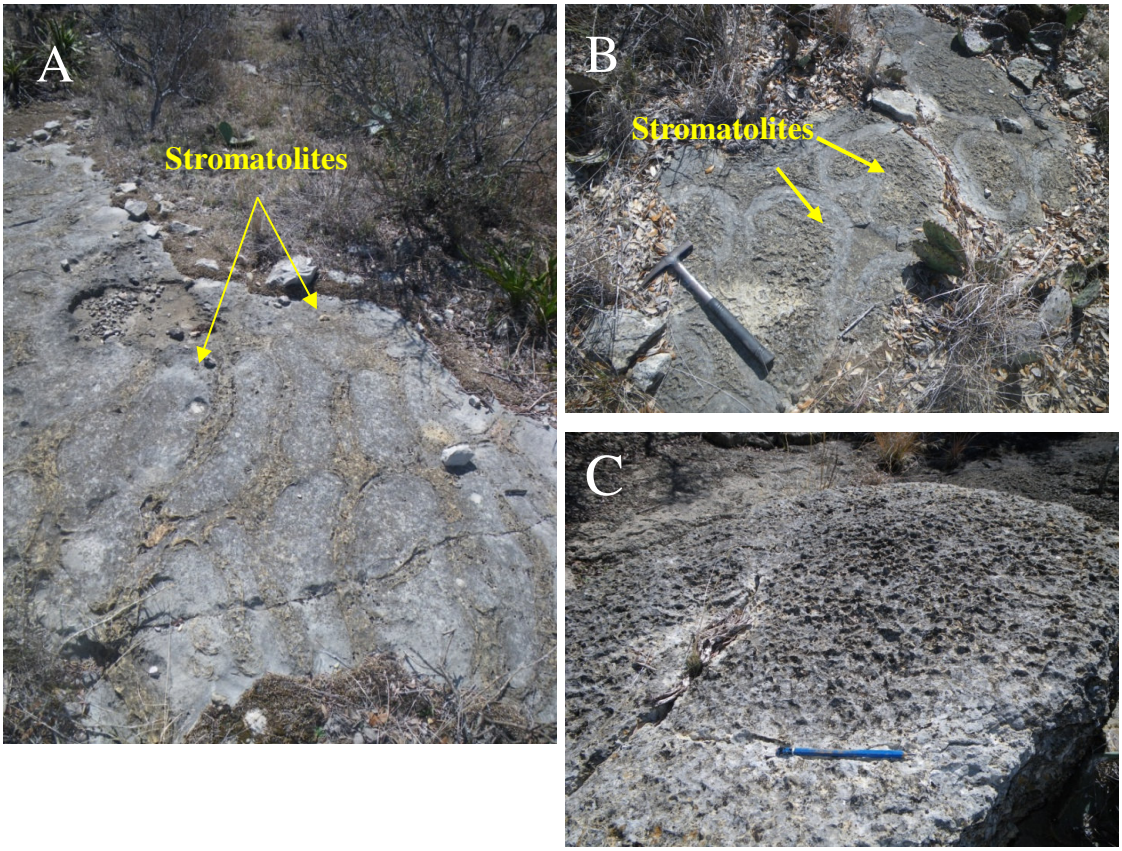

Figure 16. Stromatolites in the Point Peak limestone. Sometimes a circular pattern is present to indicate the presence of stromatolites (A & B), and other times the outcrops simply have a rough, "squiggly" pattern on the surface (C). Note pencil, hammer for scale.

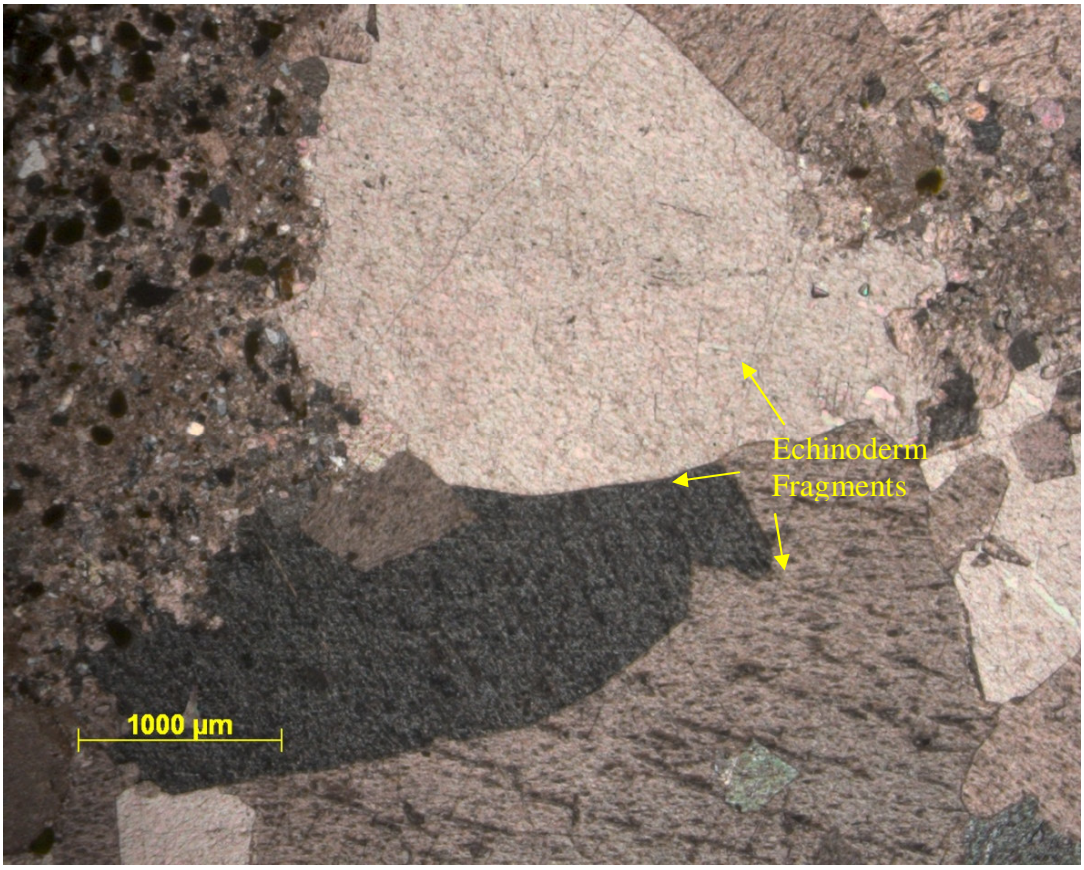

Figure 17. Thin section of the middle Point Peak limestone in natural light, showing its transition to a true calcilutite. This frame shows fragments of echinoderms, exhibiting single-crystal extinction.

At the top of the middle Point Peak is a coarse-grained, glauconitic bed. This bed is a brown-buff colored calcarenite. The grains are coarse, subrounded, and well sorted with visiblecalcite and glauconite. This bed has low porosity and is well cemented.

The upper Point Peak is a calcilutitethat is buff when fresh and weathers to blue-grey. Grains are very fine and well sorted. This is a very calcareous member which has low porosity, and high calcite cementation. Bedding is massive with a rough, irregular appearance. This member forms irregular ridges.

Above the Point Peak is the San Saba, a calcarenite. It is white, orange, and brown when fresh and weathers to brown-grey and black. Grains are coarse and well sorted. Calcite and glauconite are both very apparent. Porosity is low, becausethis member is well cemented with calcite. Bedding is massive, forms ridges. This unit is very fossiliferous (Figure 18).

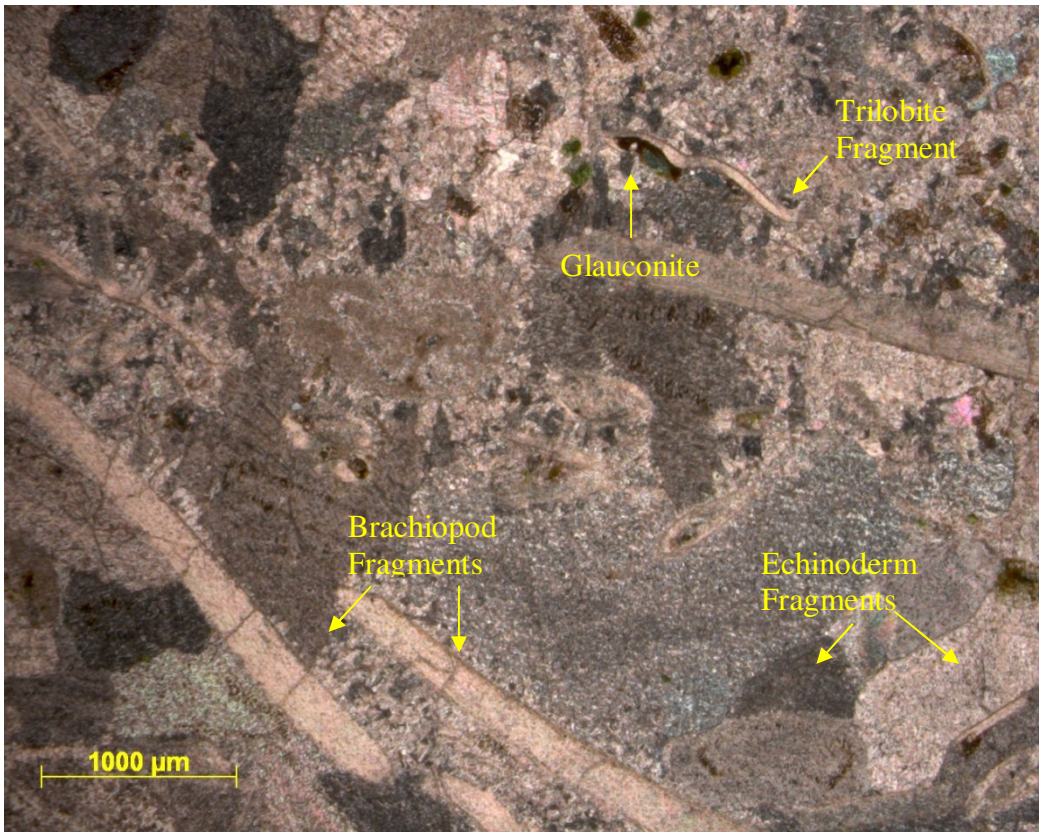

Figure 18. Thin section of the San Saba limestone in natural light, showing glauconite and fragments of trilobites, brachiopods, and echinoderms.

Near the top of the San Saba are fine-grained beds which are buff, both fresh and weathered. They have well sorted,subrounded grains that are calcareous and show low porosity and a high degree of calcite cementation.

Above the San Saba is the youngest unit investigated in this study, the Threadgill limestone. The Threadgill is a calcilutite (Figure 19) that is tan when fresh and weathers to grey-brown. Grains are very fine and well sorted. The unit is calcareous, shows low porosity, and is well cemented with calcite cement. It forms slopes. The Threadgill may show evidence of bioturbation (tunnels, burrows, etc). Often these features have been infilled with a fine, yellow sand. The Threadgill and Point Peak limestones are virtually indistinguishable in the field. Further descriptions of these units are given in the Stratigraphic Column of the Mason Area (Figure 20) and Bed-by-Bed Descriptions of Rocks of the Mason Area (Appendix A).

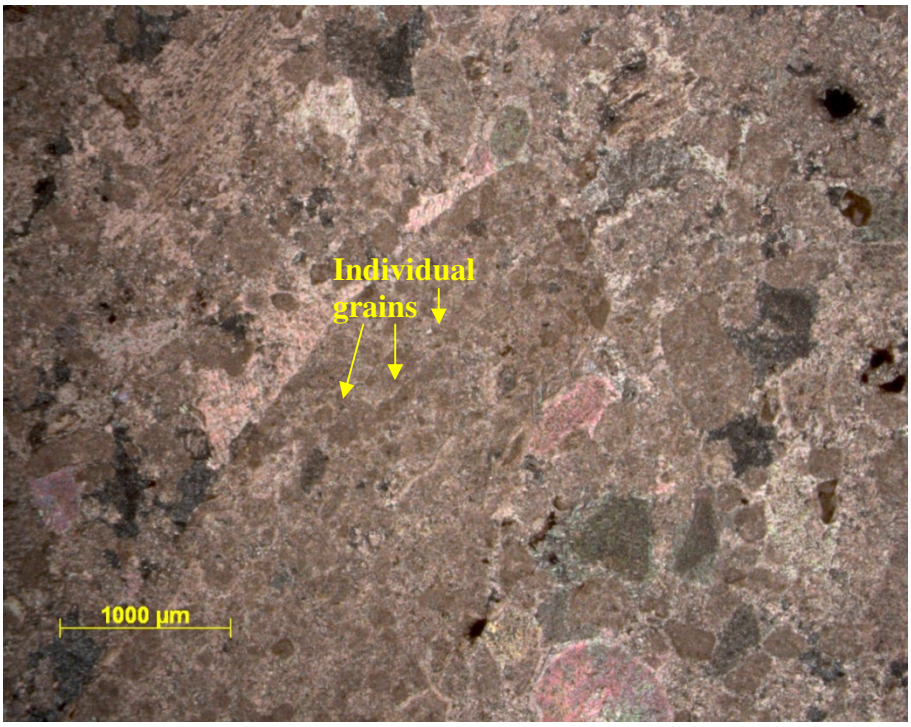

Figure 19. Thin section of the Threadgill limestone in natural light. Note very fine, well sorted grains.

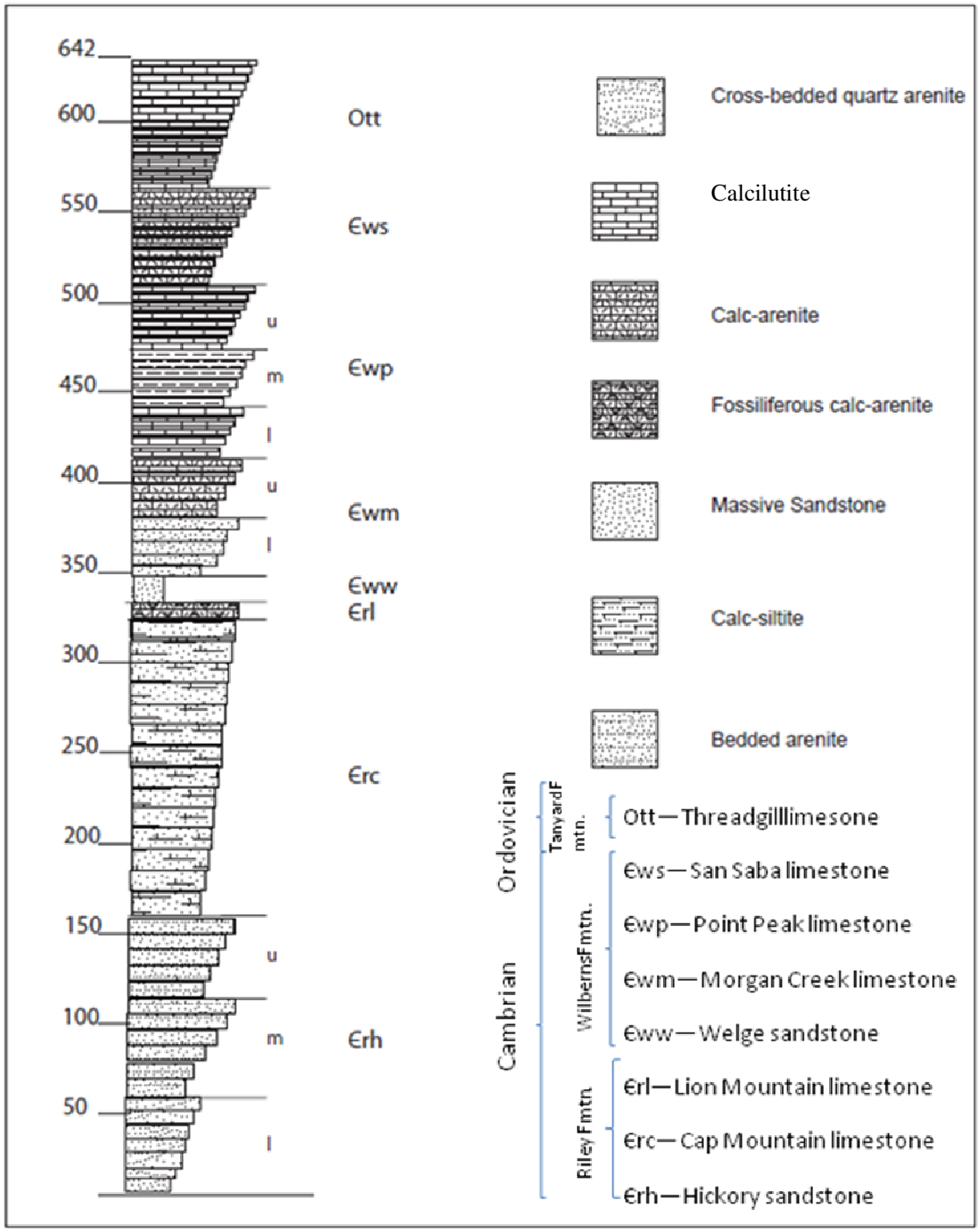

Figure 20. Stratigraphic column of units on the McMillan Ranch, beginning with the Hickory sandstone. The Hickory lies unconformably on the Precambrian basement rock. The basement rock does not outcrop on the McMillan Ranch and so is not represented in the stratigraphic column. The width of the column represents resistance to weathering. Note that most of the units become more resistant to weathering towards the top.

CHAPTER IV

THE MCMILLAN FAULT

Previous field and laboratory studies have dealt with hanging wall deformation caused by the shape of the major fault (Withjack, et al., 1995; Ellis and McClay, 1988; Gross, et al., 1997), as well as quantifying a ratio of fault length to displacement (Walsh and Watterson, 1988; Cowie and Scholz, 1992; Dawers and Anders, 1995; Kim and Sanderson, 2004). Such studies have been carried out on neighboring faults in the Mason area (Becker, 1985), but none have specifically addressed the faults on the McMillan Ranch, just to the west of the Kothmann Fault (Figure 1, page 2). This thesis gives a detailed description of the geology of the McMillan Ranch and attempts to contribute to the ongoing discussion of a ratio of fault length/displacement.

The mapping area on the McMillan Ranch has an area of ~1.2 km^2, and is bounded on all sides by fences. The main fault (McMillan Fault) is located on the far eastern side of the ranch with its hanging wall to the west. The hanging wall contains many secondary normal faults, which were mapped and analyzed, as well.

As a result of the relatively flat (some rolling hills, but none greater than 10 meters in elevation) landscape of the Mason area, the McMillan Fault was located primarily by the offset of stratigraphic units. A change in strike and dip of ~30 degrees was also observed in the rocks close to the McMillan Fault. Toward the southern end of the fault, where the Cap Mountain limestone lies adjacent to Threadgill limestone, rocks in the hanging wall progressively rotated in a counterclockwise direction, from dipping

16 degrees to the southeast to 20 degrees to the northwest, closest to the McMillan Fault. These rotated beds near the fault are accompanied by fault breccias in the Threadgill. Whereas no faults were observed in the footwall of the McMillan Fault, several minor faults occur in the hanging wall. Fault breccia is present in the Threadgill, adjacent to the McMillan Fault in the hanging wall. These brecciated zones were generally twenty meters in width.

The McMillan Fault is ~700 meters long where mapped, but extends beyond the boundaries of the mapping area to the north, with a total distance of approximately 3.7 km. Within the mapping area, a maximum stratigraphic displacement of ~300 meters is observed; this puts Cambrian-aged Cap Mountain limestone adjacent to Ordovician-aged Threadgill limestone. The McMillan Fault has an average throw of 429 meters and heave of 156 meters. The throw to length ratio on the fault is approximately 1:2. The portion of the McMillan Fault within the mapping area shows the greatest amount of throw, which is at the southern end of the fault. To the north, the fault cuts through the Hickory sandstone and is mapped by Polk (1952) as an inferred fault, setting Hickory against Hickory.

The McMillan Fault strikes approximately N10°E with its hanging wall to the northwest. Its footwall is composed primarily of the Cambrian Hickory sandstone, the overlying Cambrian Cap Mountain limestone is encountered as one travels southwestard, crossing a gradational boundary roughly two-thirds of the way down the fault.

Table 1. Structural Data of the Faults on the McMillan Ranch

F	DS	H	T	L	H/T	L/DS	L/T	L/H	Strk	Dip	DM	DNF	LNF
M	378	189	327	1120	0.58	2.96	3.43	5.93	17	west	na	na	Na
1	133	67	115	455	0.58	3.42	3.95	6.84	18	east	21	21	1120
2	21	11	18	210	0.58	10.00	11.56	20.00	5	west	84	84	1120
3	144	72	125	630	0.58	4.38	5.06	8.75	0	west	210	98	210
4	28	14	24	105	0.58	3.75	4.34	7.50	337	west	238	42	630
5	105	53	91	1400	0.58	13.33	15.41	26.67	30	west	448	49	105
6	28	14	24	630	0.58	22.50	26.01	45.00	34	west	490	84	1400
7	77	39	67	570	0.58	7.40	8.56	14.81	35	east	644	245	1300
8	42	21	36	700	0.58	16.67	19.27	33.33	30	west	665	175	1130
9	35	18	30	1300	0.58	37.14	42.94	74.29	40	east	805	175	700

In Table 1:
M = McMillan FaultStrk = Strike in Azimuth, 0=due north
DS = Dip Slip (meters) DM = Distance from McMillan Fault (meters)
H = Heave (meters) DNF = Distance from Nearest Fault (meters)
T = Throw (meters) LNF = Length of Nearest Fault (meters)
L = Length (meters) F = Fault

Within the hanging wall of the McMillan Fault are several secondary normal faults. Most of these are synthetic to the main fault, with the hanging wall to the northwest, and only three have been found that are antithetic to the main fault.

The subsidiary faults in the hanging wall of the McMillan Fault show a decrease in heave and throw with increasing distance from the McMillan Fault. Their strikes are roughly parallel to the main fault, showing a maximum rotation of approximately 40 degrees counterclockwise as one moves west, away from the main fault. After moving ~300 meters perpendicular to the main fault, strikes return to an orientation roughly parallel to the main fault. The throw to length ratio of subsidiary faults in the hanging wall of the McMillan Fault varies from 1:2 to 1:11 in the faults closest to the main fault, but increases to 1:20 with distance from the main fault. One outlier of approximately 1:40 was also calculated, but the data on this particular fault were unreliable, and so this value should likely be disregarded. This data is summarized in Table 1and in Figures 21-24, and is described in further detail in the following pages.

The first secondary fault encountered is also the first antithetic fault encountered. In the southeastern portion of the mapping area, this fault (Fault 1) occurs~130 meters west of the McMillan Fault. It strikes approximately N40°E at its southern end, but turns to roughly N05°E in its northern end. Its length is ~455 meters, though it probably continues south of the mapping area. The maximum vertical displacement of ~140 m occurs toward its southern end, where the Ordovician Threadgill limestone is set adjacent to the Cambrian Point Peak limestone and decreases toward the north. The

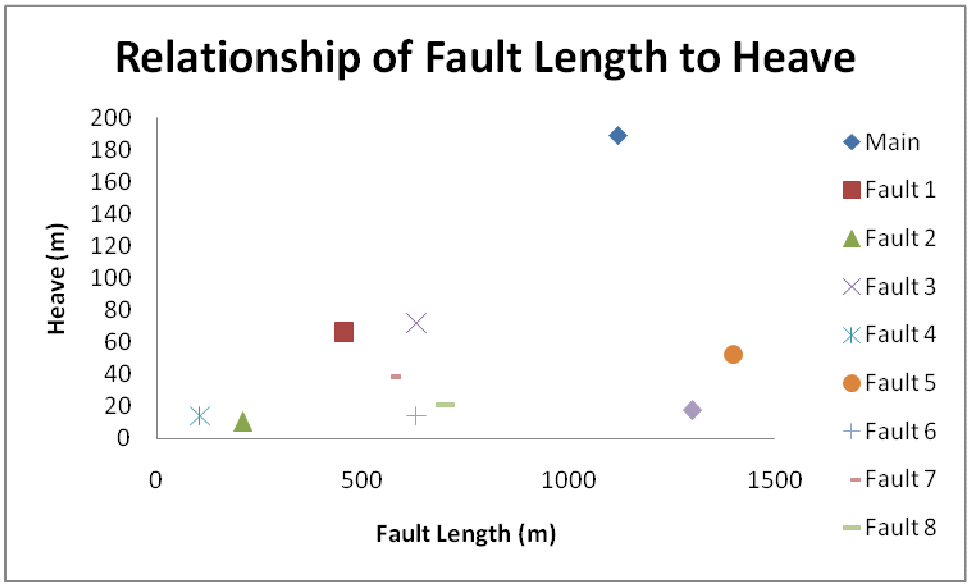

Figure 21. Scatterplot of fault length to heave on the McMillan Ranch.

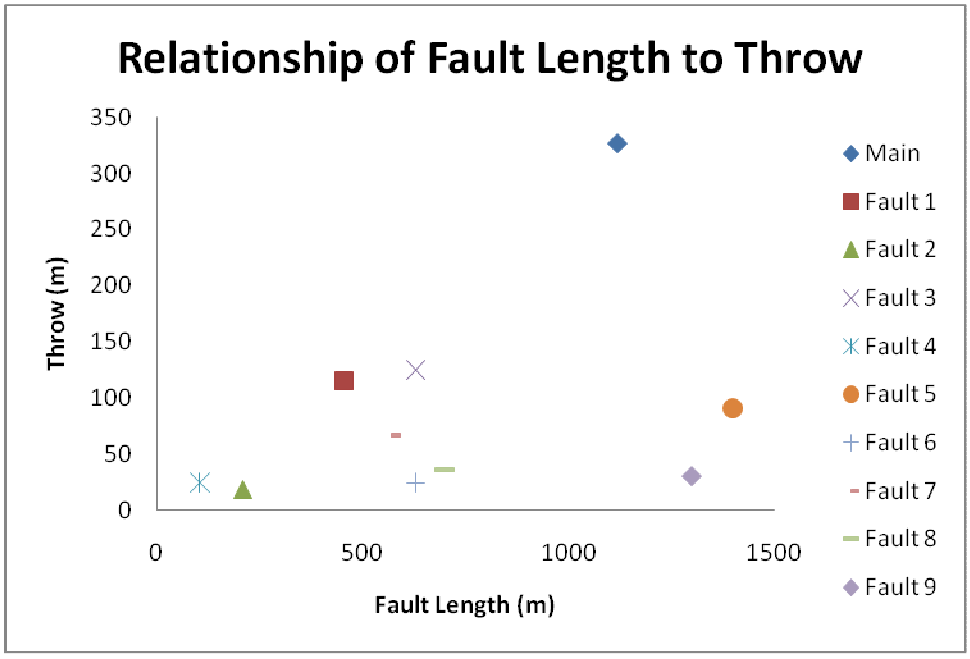

Figure 22. Scatterplot of fault length to throw on the McMillan Ranch.

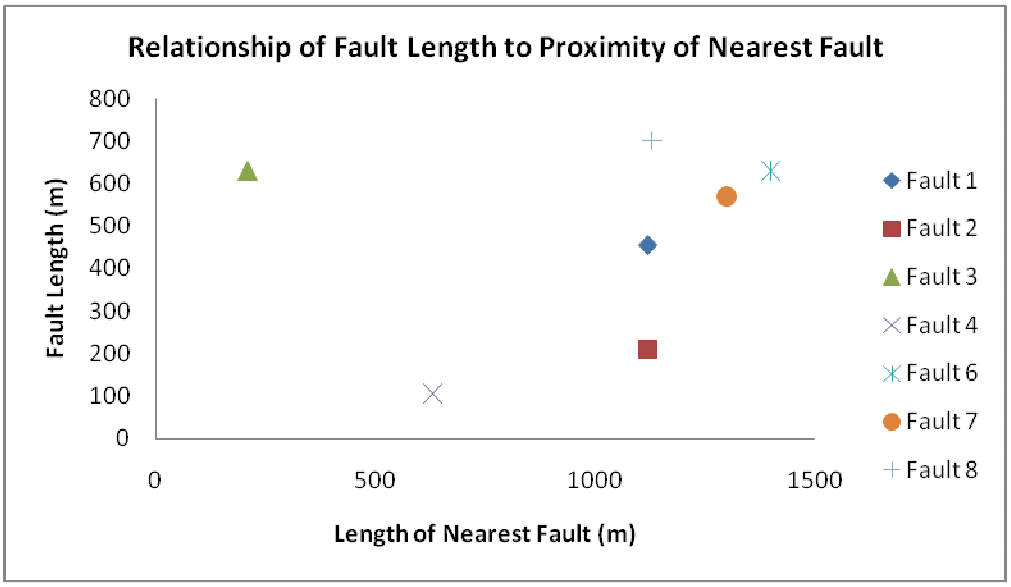

Figure 23. Scatterplot of fault length to proximity of the nearest fault. The "nearest fault" must dip towards the fault in question. Excludes the McMillan Fault and Fault 9.

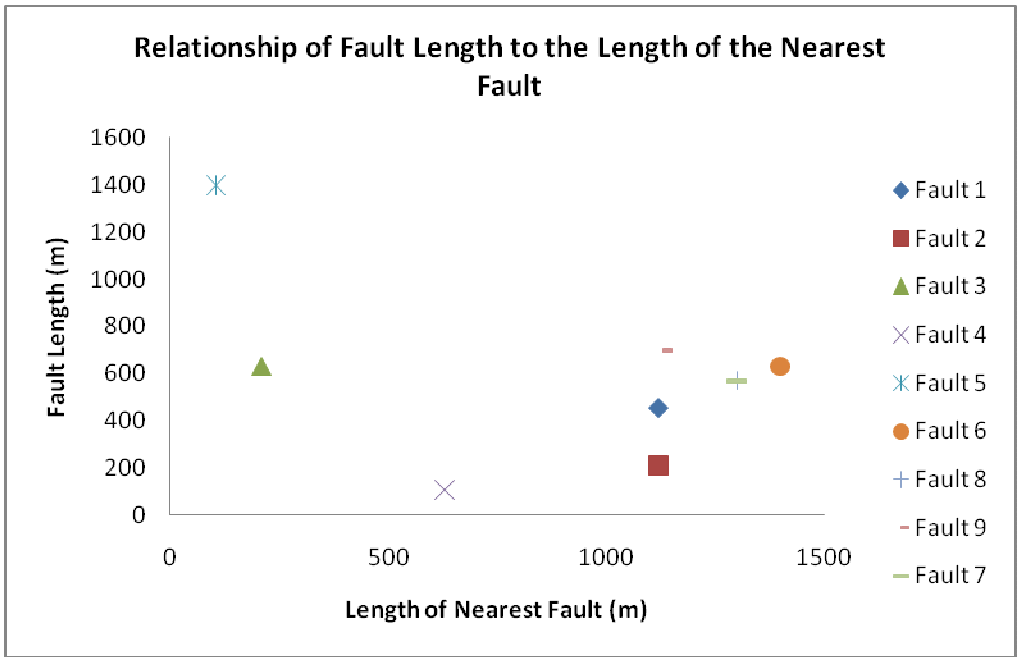

Figure 24. Scatterplot of fault length to the length of the nearest fault. This data is taken from the hanging wall of the nearest fault. Excludes the McMillan Fault.

Threadgill is subsequently found next to the Cambrian San Saba sandstone, but this is a result of the next secondary fault discussed, and is not considered when determining the maximum displacement of Fault 1.

To the west of Fault 1 are three subsequent normal faults (Fault 2, Fault 3 and Fault 4) through the Morgan Creek that cause the Morgan Creek-Point Peak stratigraphic contact to "stairstep" to the north as one travels east to west. The first is mapped as a short fault in length, but in reality may continue to the north farther than is mapped. In the north, Morgan Creek occurs on both sides of the fault,and it is difficult ascertain the extent of this fault. These faults are all synthetic to the McMillan Fault;hanging wall to the west. As far as can be determined, Fault 2 has a length of ~200 meters and a throw of ~20 meters. Fault 3 has a length of ~600 meters and a throw of ~125 meters and Fault 4 has a length of ~100 meters and throw of ~25 meters.

To the west of these "stairstepping" faults is what is believed to be another relatively long, normal fault, hanging wall to the west. It is very difficult to map because at its southern end the Point Peak limestone lies adjacent to the Threadgill limestone, and the two are nearly identical. This fault (Fault 5) is thought to be 1.0-1.4km in length. The throw is~91 meters. Three parallel normal faults are in the hanging wall, all striking roughly N30°E-N35°E. These faults are ~600-700 meters in length. The second of these three is thought to be antithetic, with its hanging wall to the east. The throw on the first of these three parallel faults (Fault 6) is ~25 meters. The throw on the next (Fault 7) is ~70 meters. The throw on the last (Fault 8) is ~35 meters.

On the westernmost side of the mapping area, another large normal fault (Fault 9) exists with its hanging wall to the west. It is thought to be ~1300 meters in length, with a throw of ~30 meters.

CHAPTER V

RESULTS AND DISCUSSION

Three categories of faults in the Mason area were described by Becker (1985): 1) major; 2) short-minor, and 3) long-minor. Major faults were segmented, generally, though not always, with straight segments. The minor faults consisted of only one segment. These faults were usually detected by the offset of stratigraphic units, though factors such as changing strike and dip, breccias and termination of bedding occurred as well.

The density of minor faults is dependent on the lithology and structural position, with more minor faults in the Mason fault hanging wall than in the footwall (Becker, 1985). The McMillan Fault, just west of Mason, appears to be of the major, segmented variety.

The mapping area contains only one segment of this fault. At the northern end, Hickory sandstone lies next to Morgan Creek limestone. At the southern end, after a gradational boundary in the footwall, Cap Mountain limestone lies next to Threadgill limestone (Figure 25). To the north, out of the mapping area, however, is another Hickory/Cap Mountain contact. This Cap Mountain is located updip of the Hickory sandstone just to the south. This implies another fault in very close proximity to the McMillan Fault.

As a result of the relatively flat (some rolling hills, but none over ~10 meters in elevation) landscape of the Mason area, the McMillan Fault was located primarily by the offset of stratigraphic units, as described by Becker (1985) and in the findings of this study. A dramatic change in strike and dip was also encountered in the rocks close to the McMillan Fault (Figure 26).

Toward the southern end of the fault, where the Cap Mountain lies adjacent to Threadgill, rocks in the hanging wall progressively rotate in a counterclockwise direction, from dipping 16 degrees to the southeast to 20 degrees to the northwest, closest to the McMillan Fault (Figure 27). These rotated beds near the fault are accompanied by fault breccias in the Threadgill (Figure 28). Whereas no faults were observed in the footwall of the McMillan Fault, several minor faults occur in the hanging wall.

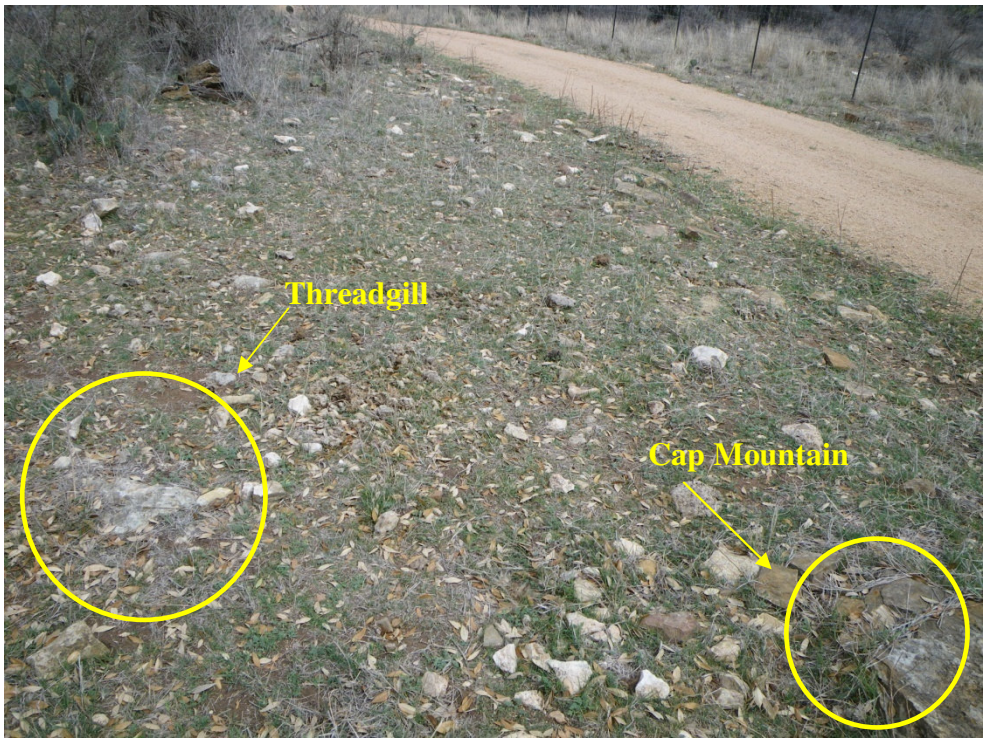

Figure 25. The McMillan Fault: Threadgill sits adjacent to Cap Mountain in the southern portion of the mapping area.

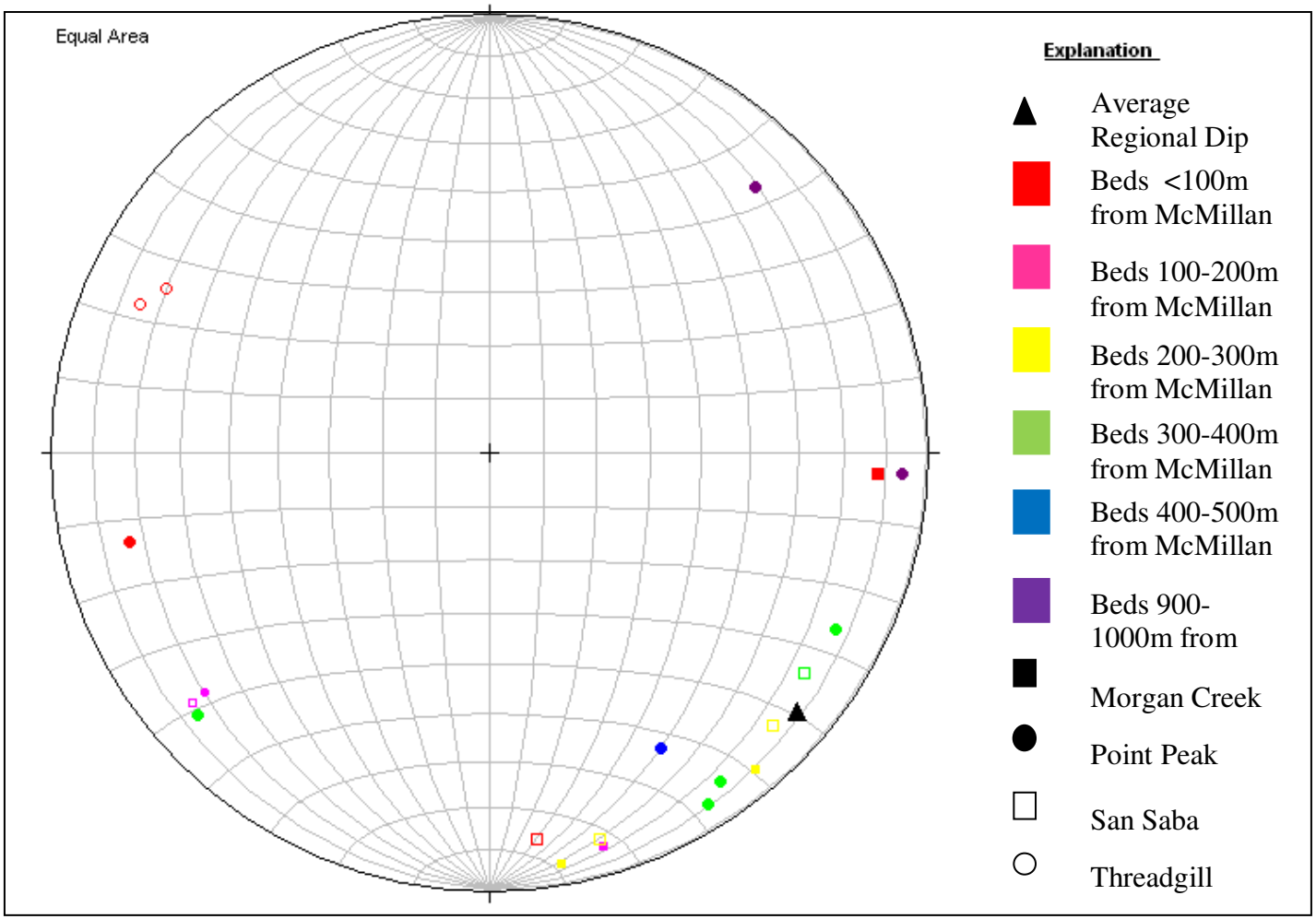

Figure 26. Stereonet showing the regional dip and dip direction of the units in the Mason area and the dips and dip directions of the rocks on the McMillan Ranch. Note the rotation of beds with proximity to the McMillan Fault.

Figure 27. Rotated bed of Threadgill limestone, ~10 meters from the McMillan Fault. Regional dip is 9-10 degrees to the southeast, and this bed dips ~20 degrees to the northwest.

Figure 28. Fault breccia in the Threadgill limestone in the southern portion of the mapping area. Watch for scale.

Withjack and others (1995) performed a series of experiments using clay models to determine the effect of the shape of the footwall on minor faults found in the hanging wall. They determined that a footwall with a straight fault surface, at an angle of 45 degrees, ultimately caused few faults antithetic to the main fault, located closest to the main fault and a majority of synthetic faults with distance from the main fault. This pattern is observed at the McMillan Ranch. Other experiments produced minor faults that were predominantly anithetic to the main fault, even with increasing distance. Strike and dip data, which demonstrate the rotation of beds away from the footwall with increasing proximity to the McMillan Fault imply the presence of a drag fold. This has been observed at other faults in the Mason area (Becker, 1985) and is often associated with listric faults (Hamblin, 1965; Crans, et. al, 1980). It is possible, however, for drag folds to occur in non-listric faults (Angelier, 1979; Patton, 1984), typically if the faults are planar in the basement rock and steepen upwards (Becker, 1985). This is likely the case for the McMillan Fault. Listric faults are commonly accompanied by rollover anticlines (Mercki, 1972), and no such structure is found near the McMillan Fault.

As demonstrated in Table 1 (page 41) and in Figures 21-24 (pages 43-44), a single length-displacement ratio for the faults on the McMillan Ranch was not determined, just as in previous studies (Walsh and Watterson, 1988; Cowie and Scholz, 1992; Dawers and Anders, 1995; Kim and Sanderson, 2004). The ratios determined clustered into a range primarily from 1:3 to 1:8 for length to throw ratios, with one as high as 1:20. Fault 9 had a length to throw ratio of 1:42, but considering the difficulty with which this fault was located and the uncertainty of its accuracy, this value should be

disregarded. When dip-slip is considered, ratios ranged from 1:3 to 1:20. Strike-slip in the Mason area is negligible (Becker, 1985). Ratios of length to heave ranged from 1:5 to 1:30 and above.

As shown in the Geologic Map of the McMillan Ranch in Mason, Texas (Figure 29), and the Cross Section of the McMillan Ranch in Mason, Texas (Figure 30) three long normal faults run through the mapping area. The one with the greatest amount of displacement associated with it is the McMillan Fault on the far eastern side of the mapping area. The other two faults roughly parallel the McMillan Fault, but are poorly constrained. These faults show a significantly lower amount of displacement for their lengths, as far as can be determined. It is worth noting, however, that just as was observed by Becker (1985), significant deformation in the form of secondary faults is found in the hanging walls of these faults, not the footwalls. The deformation in the footwall of the second main fault (Fault 5) is thought to be a result of movement along the McMillan Fault. Fault 5 is likely a result of the McMillan Fault. In the smaller secondary faults, the hanging walls had the most fractures (Figures 31 and 32).

The McMillan Fault has a length to throw and length to heave ratio which is far greater than the other faults in the mapping area. Further research, perhaps focusing on the effect of different lithologies on length-displacement ratio, is needed. The length of secondary faults based upon the length and proximity of the nearest fault which dips towards it is far more predictable, following a very nearly linear pattern of growth (Figures 23 and 24, page 44).

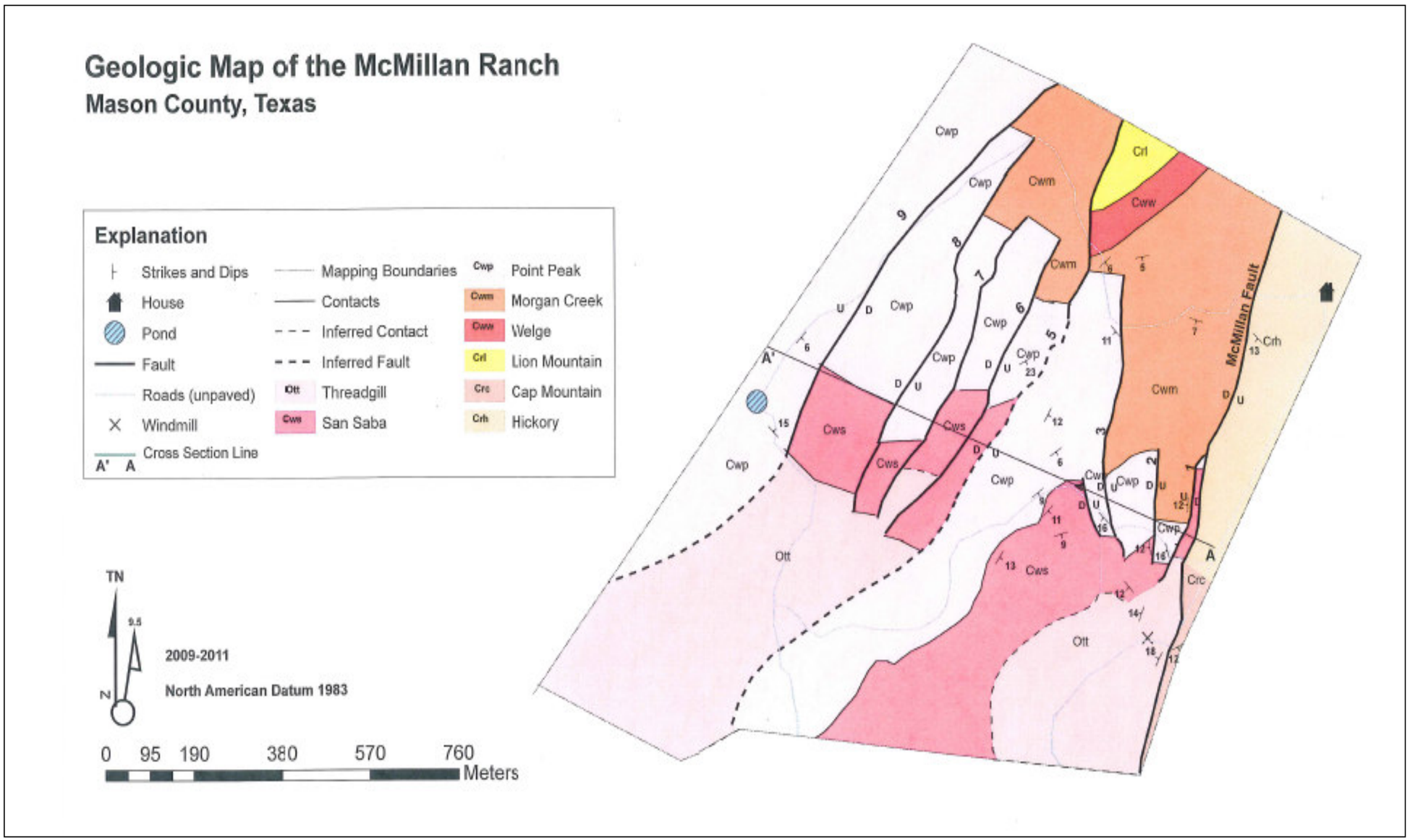

Figure 29. Geologic Map of the McMillan Ranch in Mason, Texas.

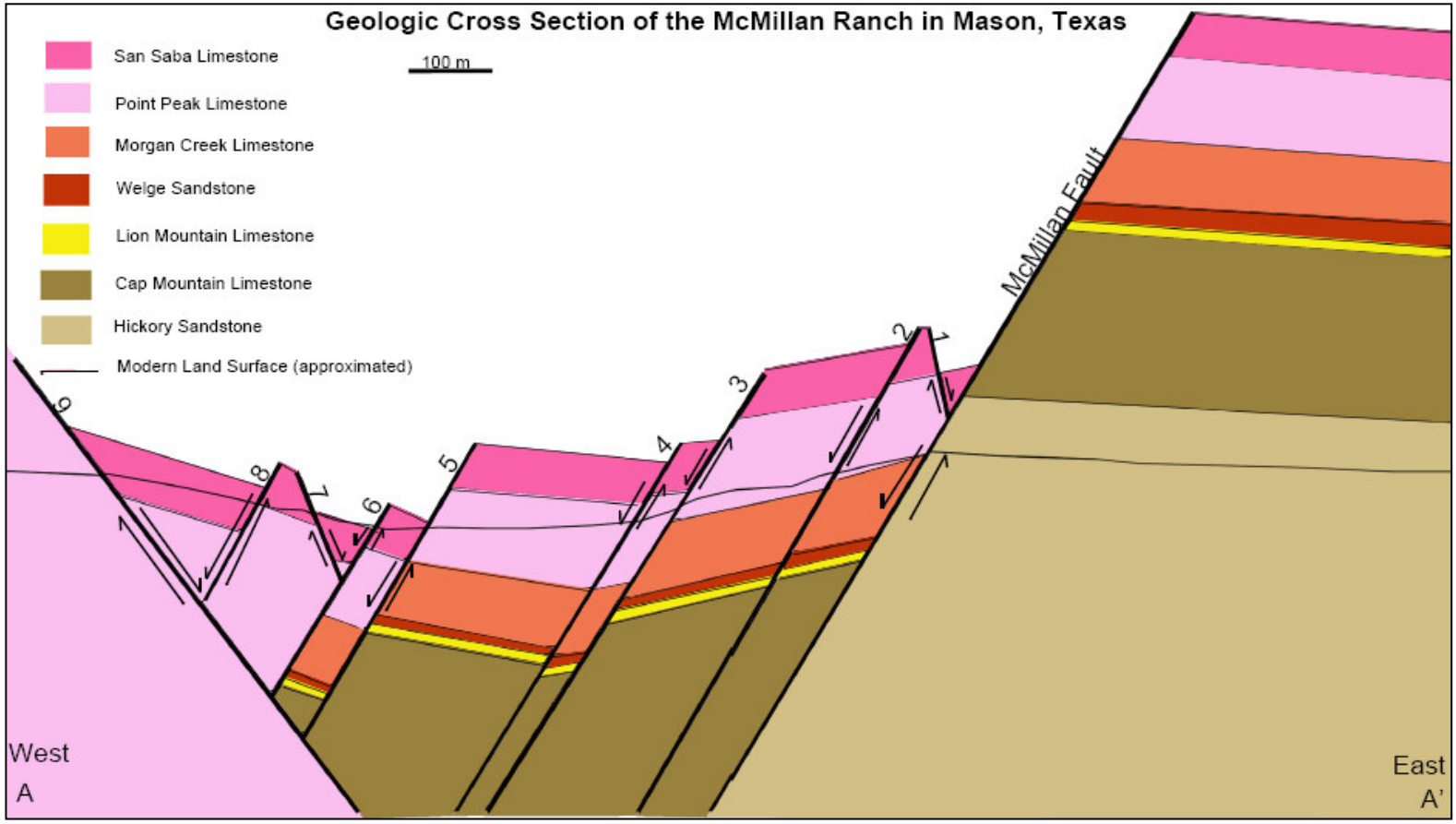

Figure 30. Restoreded cross section of the McMillan Ranch in Mason, Texas. The Point Peak on the western edge of the cross section appears thicker than in other places because of the rotation of beds. The Point Peak on the western edge has been rotated so that the cross section line is perpendicular to dip, making the Point Peak there appear very thick (the bed is dipping "into" the page.

Figure 31. Fractured Threadgill limestone from the hanging wall of the McMillan Fault. The most fractured outcrops were generally found in the hanging walls of all the faults on the McMillan Ranch.

Figure 32. Intact San Saba adjacent to fractured Threadgill. Dashed line represents approximate location of fault.

A definite trend is noted of deformation in the hanging wall of each fault, regardless of length or of displacement, which exceeds the deformation in the footwall. It is thought that the McMillan Fault is planar, based upon the orientation of faults in the hanging wall.

CHAPTER VI

CONCLUSIONS

The McMillan Ranch was mapped at a scale of 1:7,000. The resulting map was then used to perform basic structural analysis and attempt to determine a ratio of fault length to displacement which could then be applied to all faults in the area. A detailed stratigraphy study was carried out, including bed-by-bed descriptions and thin sections.

The nature of the normal faults in the Mason area varies depending on length, lithology, and proximity to other faults. Therefore, a single length/displacement ratio that can be applied to all faults could not be determined. This thesis was able to show the heterogeneity of the faults in the area, and how they are affected by various factors such as length, proximity to other faults, and length of nearby faults. The geologic map of the McMillan Ranch and cross section of the McMillan Ranch show the complex nature of these fault systems at a larger scale than most maps of the area have previously done, and implies that the large faults shown on previous maps of the Mason Area are actually systems of several, small faults. This was previously implied by Becker (1985). The bed-by-bed descriptions and thin sections provide more detailed descriptions of the units so that future studies of the Mason area, and the faults in it that displace units by only a few meters instead of hundreds of meters, can be studied further.

The study area was selected because it contains a great number of faults of various lengths in a small area, and had opportunities to study faults of different lengths that were all affected by the same geologic phenomena. A scale of 1:7,000 was chosen

because it best showed the McMillan Fault and many of its subsidiary faults. There are still smaller faults that could not be represented even at a scale of 1:7,000, and so there is still potential for doing further research at an even larger scale.

Mapping became much easier once a solid understanding of the many beds in the units was gained. The bed-by-bed descriptions provided clarification of the lithologies that were being mapped: originally, the ranch was being mapped based upon simple, generalized descriptions of the units. This proved insufficient for the magnitude of the project. After understanding the variations of each unit and where they were located relative to one another, mapping became much easier.

The purpose of this study was to show the complexity of the geology of Mason, as an area of interest for structural geologists and sedimentologists, and to contribute to the search for a length to displacement ratio for normal faults in general. The map and sedimentary descriptions, including the bed-by-bed descriptions convey the complexity of the area and the variations possible within even one unit of rock. The structural data gathered from the field convey the varying natures of faults, even within the same area, and support the conclusion that length alone is not sufficient to predict displacement value on a fault.

A fundamental error upon beginning this study was the assumption of a homogeneous Earth. The idea that math can be used to predict the heave or throw of a normal fault simply based upon its length assumes that rocks behave in a homogeneous manner and can be expected to follow rules based upon an “if this, then that” premise. As the earth is heterogeneous, this assumption was flawed and the observations that followed

only showed that no single fault length to displacement ratio could be determined for all the normal faults in the Mason area. It may be possible to consider each individual unit homogeneous and predict how shallow faults that only exist in one unit without cross-cutting others behave, but this would not be possible in Mason. This is a problem in other studies, as well. In previous studies of this nature, the underlying assumption is that the fault must behave in a predictable manner, and it is the job of the scientist to decipher the relationship between the different attributes of the fault. As long as the faults are in different lithologies, however, the assumption of their homogeneity is faulty.

REFERENCES CITED

Angelier, J., 1979, Determination of the mean principal directions of stresses for a given fault population: Tectonophysics, v. 56, T17-T26.

Barnes, V.E., 1981, Llano Sheet, Austin, Texas: Bureau of Economic Geology, scale 1:250,000, 1 sheet.

Becker, J.E., 1985, Structural Analysis of the Western Llano Uplift with Emphasis on the Mason Fault, M.S. Thesis: Texas A&M University.

Carlson, W.D., 1998, Petrologic constraints on the tectonic evolution of the Llano uplift, *in*. Gilbert, M.C. and Hogan, J.P., Basement Tectonics, Springer: New York, 3-27.

Chafetz, H.S., 1980, Evidence for an arid to semi-arid climate during deposition of the Cambrian system in central Texas, USA: Palaeogeography, Palaeoclimatology, Palaeoecology, v. 30, 83-95.

Cowie, P.A. and Scholz, C.H., 1992, Displacement-length scaling relationship for faults: data synthesis and discussion: Journal of Structural Geology, v. 14, 1149-1156.

Crans, W., Mandl, G., and Haremboure, J., 1980, On the theory of growth faulting: a geomechanical delta model based on gravity sliding: Journal of Petroleum Geology, v. 2, 265-307.

Dawers. N.H. and Anders, M.H., 1995. Displacement-length scaling and fault linkage: Journal of Structural Geology, v.17, 607-614.

Ellis, P.G and McClay, K.R., 1988, Listric extensional fault systems—results of analogue model experiments:Basin Research, v. 1, 55-70

Ewing, T.E., 2005, Phanerozoic development of the Llano uplift: Bulletin of the South Texas Geological Society, v. 45.

Gross, M.R., Bahat, D., and Becker, A., Relations between jointing and faulting based on fracture-spacing ratios and fault-slip profiles: a new method to estimate strain in layered rocks: Geology, v. 25, 887-890.

Hamblin, W.K., 1965, Origin of "reverse drag" on the downthrown side of normal faults: Geological Society of America Bulletin, v. 76, 1145-1164.

Kim, Y. and Sanderson, D.J., 2004, The relationship between displacement and length of faults: a review: Earth-Science Reviews, v.68, 317-334.

Mercki, P., 1972, Structural geology of the Cenozoic Niger delta, *in* Dessauvagie, F.F.J. and Whiteman, A.J., African Geology: Nigeria, Springer: New York, 636-646.

Mosher, S., 1998, Tectonic evolution of the southern Laurentian Grenville Orogenic Belt: Bulletin of the Geological Society of America, v. 110, 1357-1375.

Mosher, S., 2008, Mesoproterozoic plate tectonics: A collisional model for the Grenville-aged orogenic belt in the Llano uplift, central Texas: Geology, v. 36, 55-58.

Patton, T.L., 1984, Normal-fault and fold development in sedimentary rocks above a preexisting basement normal fault, Ph.D. dissertation: Texas A&M University.

Polk, T.P., 1952, Geology of the West Mason Area, Texas, M.S. Thesis: Texas A&M University

Rives, T., Razack, M., Petit, J.P. and Rawnsley, K.D., 1992, Joint spacing: analogue and numerical simulations: Journal of Structural Geology, v. 14, 925-937.

Singhurst, J.R., Sanchez, L.L., Frels, D., Schwertner, T.W., Mitchell, M., Moren, S., and Holmes, W.C., 2007, The vascular flora of Mason Mountain Wildlife Management Area, Mason County, Texas: Southeastern Naturalist, v.6(4), 683-692.

Smith, R.K. and Gray, W., 2009, Evolution by replenishment fractional crystallization (RFC) of midproterozoic magmatic enclaves in granites of the eastern Llano uplift, central Texas, USA: American Geophysical Union Fall Meeting Abstracts.

Smith, R.K., Gray, W., Gibbs, T., and Gallegos, M.A., 2010, Petrogenesis of mesoproterozoic granitic plutons, eastern Llano uplift, central Texas, USA: Lithos, v. 118, 238-254.

Walsh, J.J. and Watterson, J. 1988, Analysis of the relationship between displacements and dimensions of faults: Journal of Structural Geology, v.10, 239-247.

Withjack, M.O., Islam, Q.T. and La Pointe, P.R., 1995, Normal faults and their hanging-wall deformation: an experimental study: American Association of Professional Geologists, v. 79, 1-18.

APPENDIX A

Bed-by-Bed Descriptions of the Rocks in the Mason Area Beginning with the Lion Mountain

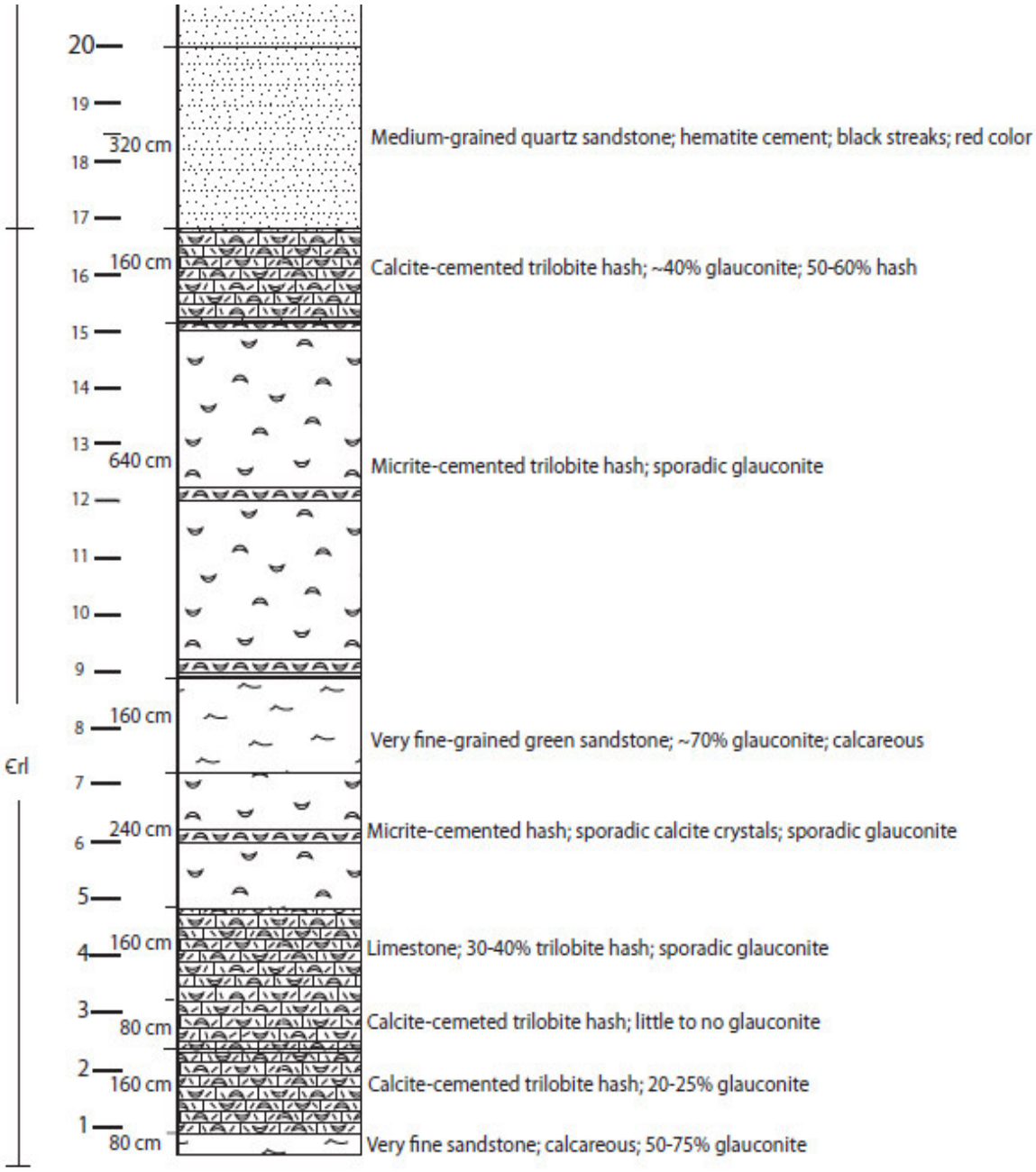

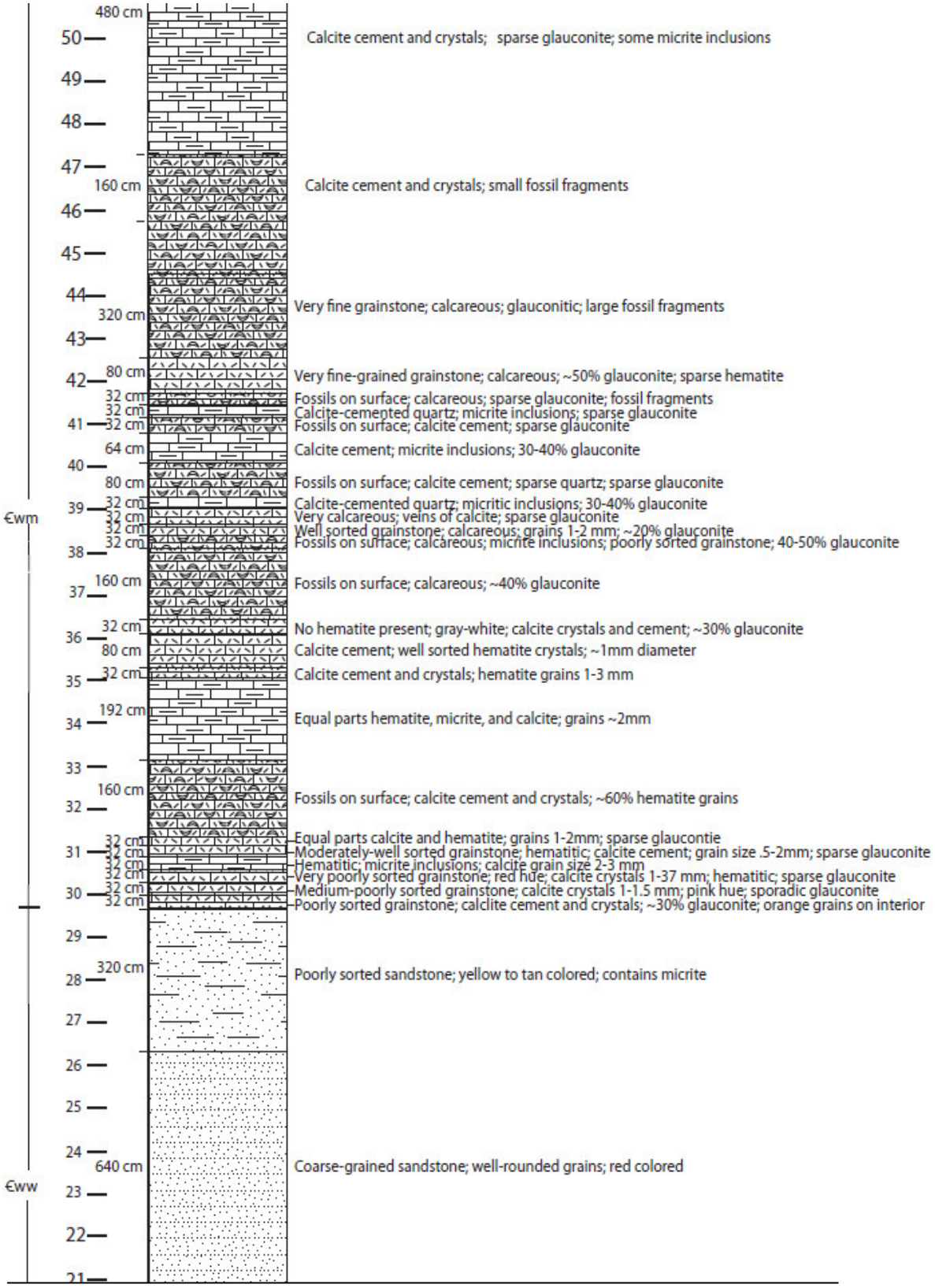
480 cm
50
49
48
47
160 cm
46
45
44
320 cm
43
80 cm
42
32 cm
32 cm
41
32 cm
64 cm
40
80 cm
32 cm
39
32 cm
32 cm
32 cm
38
160 cm
37
32 cm
36
80 cm
32 cm
35
192 cm
34
33
160 cm
32
32 cm
32 cm
31
32 cm
32 cm
32 cm
30
32 cm
29
320 cm
28
27
26
25
24
640 cm
23
22
21
€wm
€ww
Calcite cement and crystals; sparse glauconite; some micrite inclusions
Calcite cement and crystals; small fossil fragments
Very fine grainstone; calcareous; glauconitic; large fossil fragments
Very fine-grained grainstone; calcareous; ~50% glauconite; sparse hematite
Fossils on surface; calcareous; sparse glauconite; fossil fragments
Calcite-cemented quartz; micrite inclusions; sparse glauconite
Fossils on surface; calcite cement; sparse glauconite
Calcite cement; micrite inclusions; 30-40% glauconite
Fossils on surface; calcite cement; sparse quartz; sparse glauconite
Calcite-cemented quartz; micritic inclusions; 30-40% glauconite
Very calcareous; veins of calcite; sparse glauconite
Well sorted grainstone; calcareous; grains 1-2 mm; ~20% glauconite
Fossils on surface; calcareous; micrite inclusions; poorly sorted grainstone; 40-50% glauconite
Fossils on surface; calcareous; ~40% glauconite
No hematite present; gray-white; calcite crystals and cement; ~30% glauconite
Calcite cement; well sorted hematite crystals; ~1mm diameter
Calcite cement and crystals; hematite grains 1-3 mm
Equal parts hematite, micrite, and calcite; grains ~2mm
Fossils on surface; calcite cement and crystals; ~60% hematite grains
Equal parts calcite and hematite; grains 1-2mm; sparse glaucontie
Moderately-well sorted grainstone; hematitic; calcite cement; grain size .5-2mm; sparse glauconite
Hematitic; micrite inclusions; calcite grain size 2-3 mm
Very poorly sorted grainstone; red hue; calcite crystals 1-37 mm; hematitic; sparse glauconite
Medium-poorly sorted grainstone; calcite crystals 1-1.5 mm; pink hue; sporadic glauconite
Poorly sorted grainstone; calclite cement and crystals; ~30% glauconite; orange grains on interior
Poorly sorted sandstone; yellow to tan colored; contains micrite
Coarse-grained sandstone; well-rounded grains; red colored

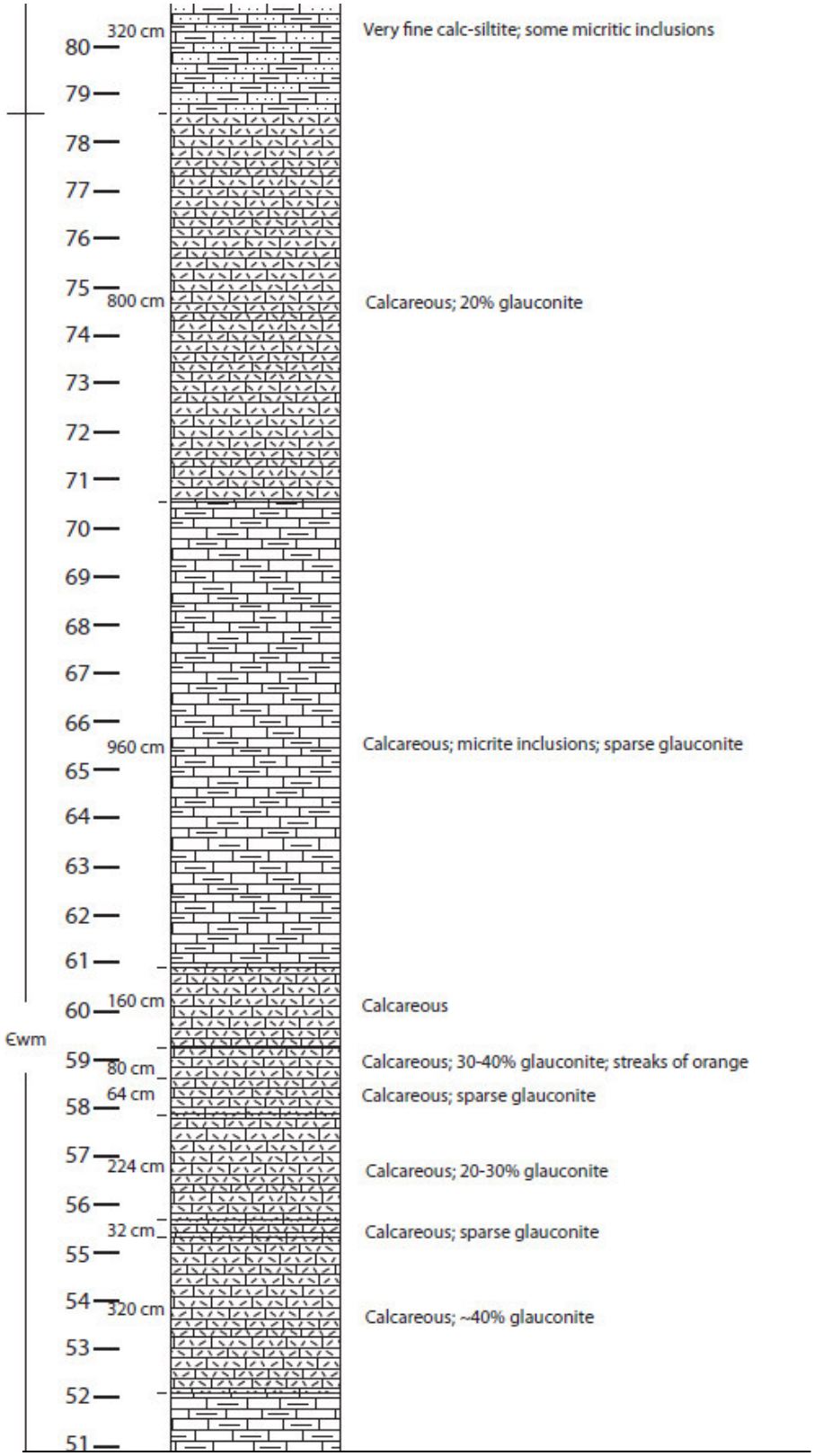
320 cm
Very fine calc-siltite; some micritic inclusions
800 cm
Calcareous; 20% glauconite
960 cm
Calcareous; micrite inclusions; sparse glauconite
160 cm
Calcareous
Ewm
80 cm
Calcareous; 30-40% glauconite; streaks of orange
64 cm
Calcareous; sparse glauconite
224 cm
Calcareous; 20-30% glauconite
32 cm
Calcareous; sparse glauconite
320 cm
Calcareous; ~40% glauconite
80
79
78
77
76
75
74
73
72
71
70
69
68
67
66
65
64
63
62
61
60
59
58
57
56
55
54
53
52
51

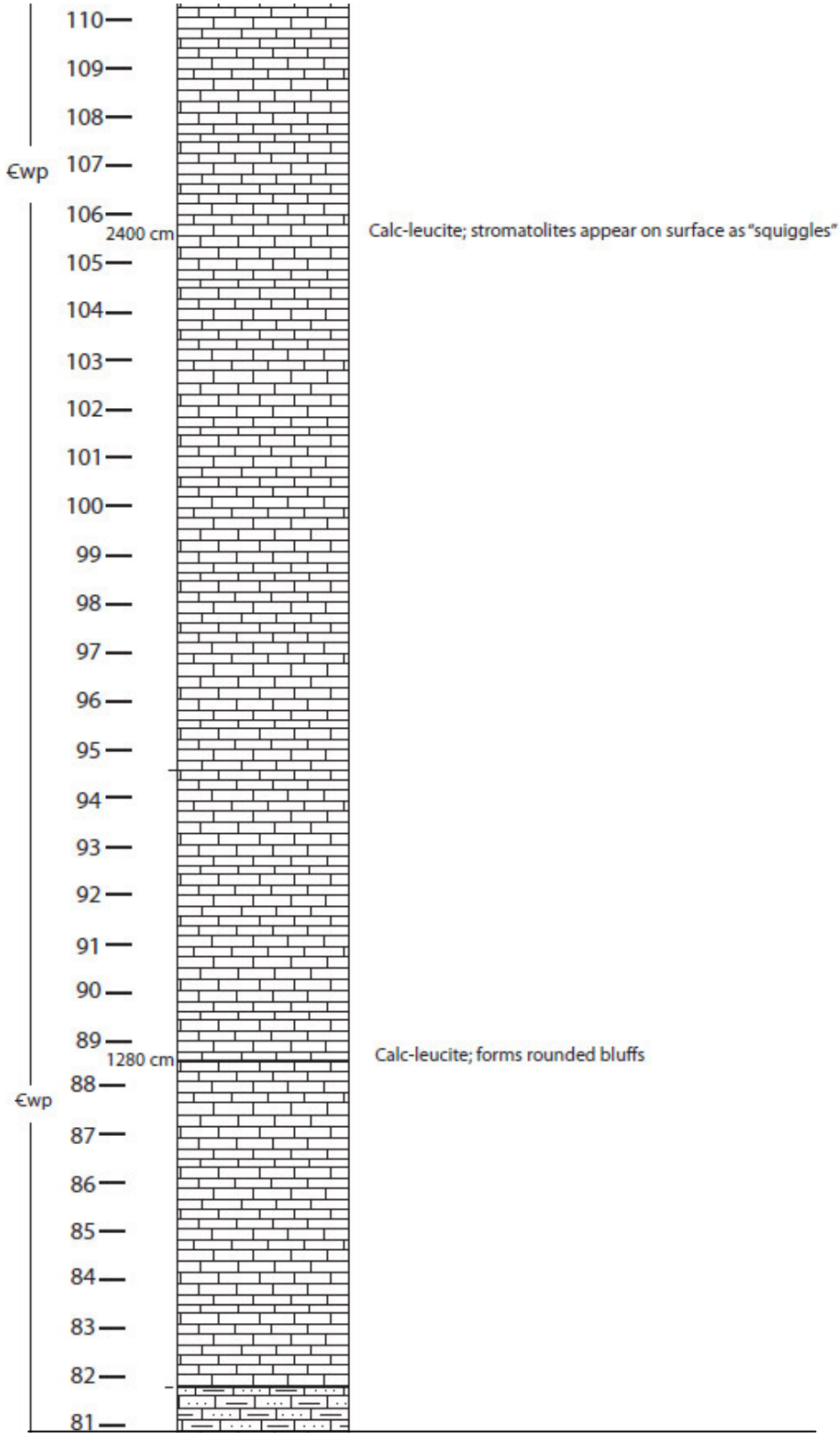
110
109
108
€wp
107
106
2400 cm
105
104
103
102
101
100
99
98
97
96
95
94
93
92
91
90
89
1280 cm
€wp
88
87
86
85
84
83
82
81
Calc-leucite; stromatolites appear on surface as "squiggles"
Calc-leucite; forms rounded bluffs

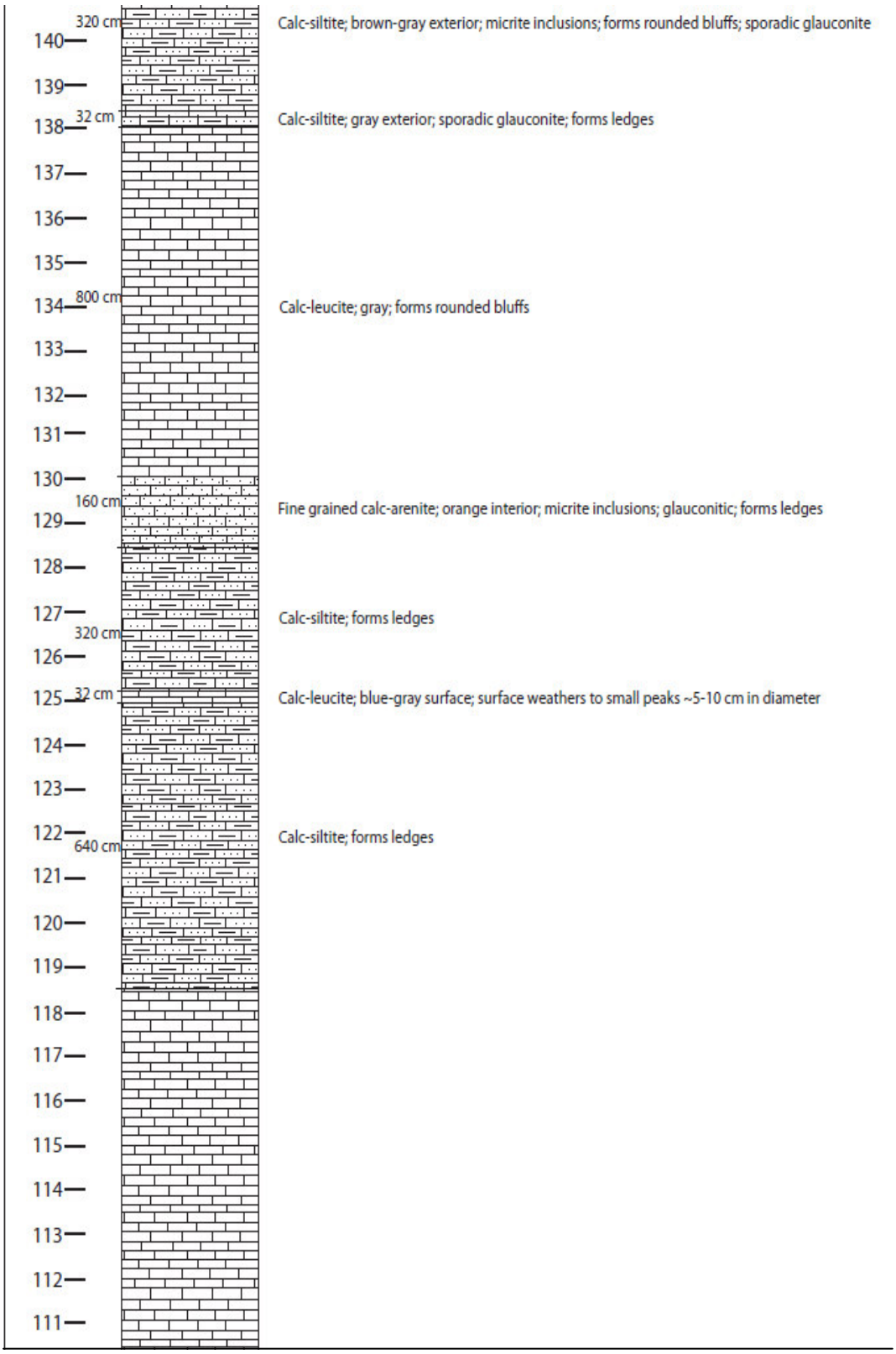
320 cm
140
139
32 cm
138
137
136
135
800 cm
134
133
132
131
130
160 cm
129
128
127
320 cm
126
32 cm
125
124
123
122
640 cm
121
120
119
118
117
116
115
114
113
112
111
Calc-siltite; brown-gray exterior; micrite inclusions; forms rounded bluffs; sporadic glauconite
Calc-siltite; gray exterior; sporadic glauconite; forms ledges
Calc-leucite; gray; forms rounded bluffs
Fine grained calc-arenite; orange interior; micrite inclusions; glauconitic; forms ledges
Calc-siltite; forms ledges
Calc-leucite; blue-gray surface; surface weathers to small peaks ~5-10 cm in diameter
Calc-siltite; forms ledges

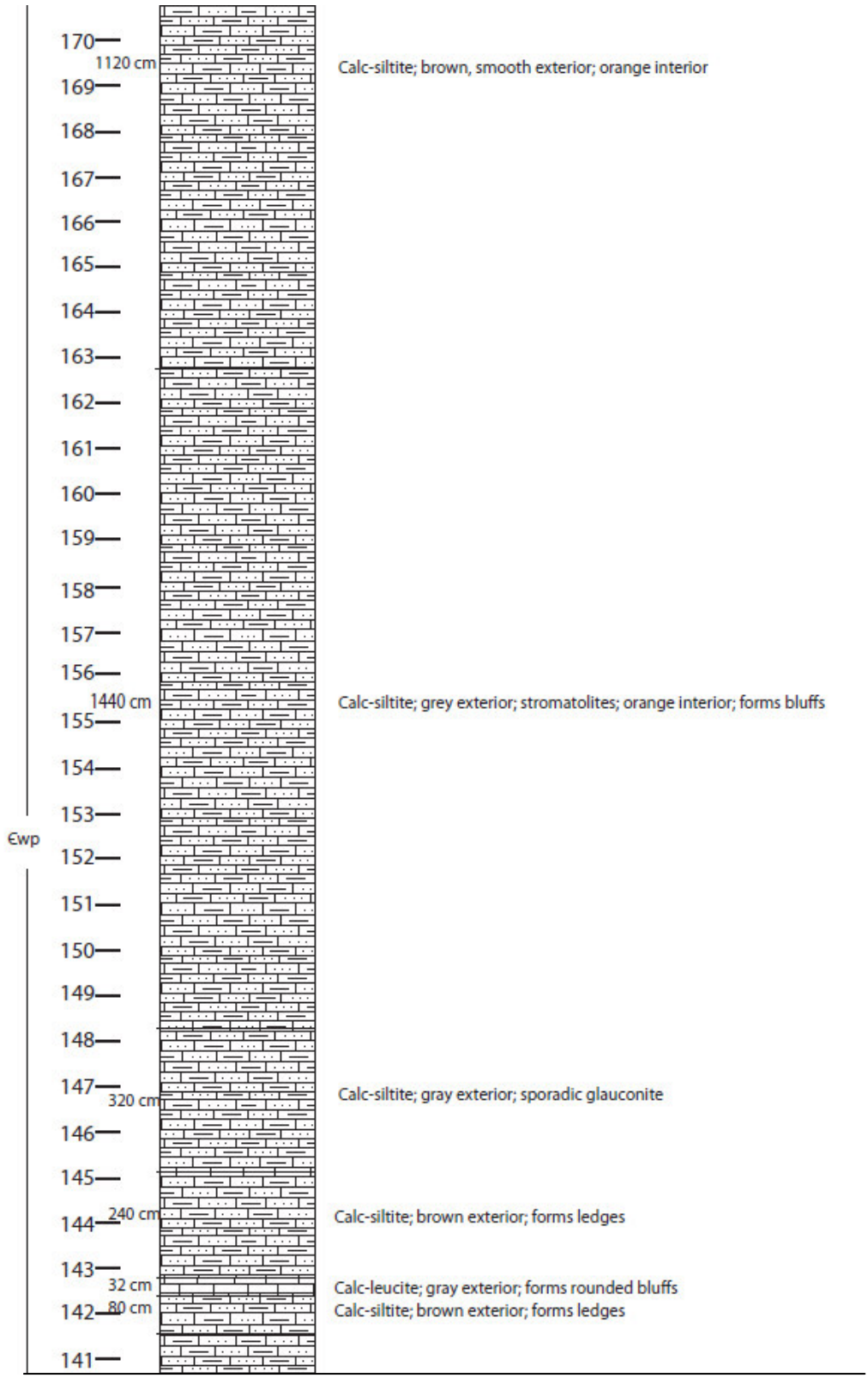
170
1120 cm
169
168
167
166
165
164
163
162
161
160
159
158
157
156
1440 cm
155
154
153
Ewp
152
151
150
149
148
147
320 cm
146
145
240 cm
144
143
32 cm
80 cm
142
141
Calc-siltite; brown, smooth exterior; orange interior
Calc-siltite; grey exterior; stromatolites; orange interior; forms bluffs
Calc-siltite; gray exterior; sporadic glauconite
Calc-siltite; brown exterior; forms ledges
Calc-leucite; gray exterior; forms rounded bluffs
Calc-siltite; brown exterior; forms ledges

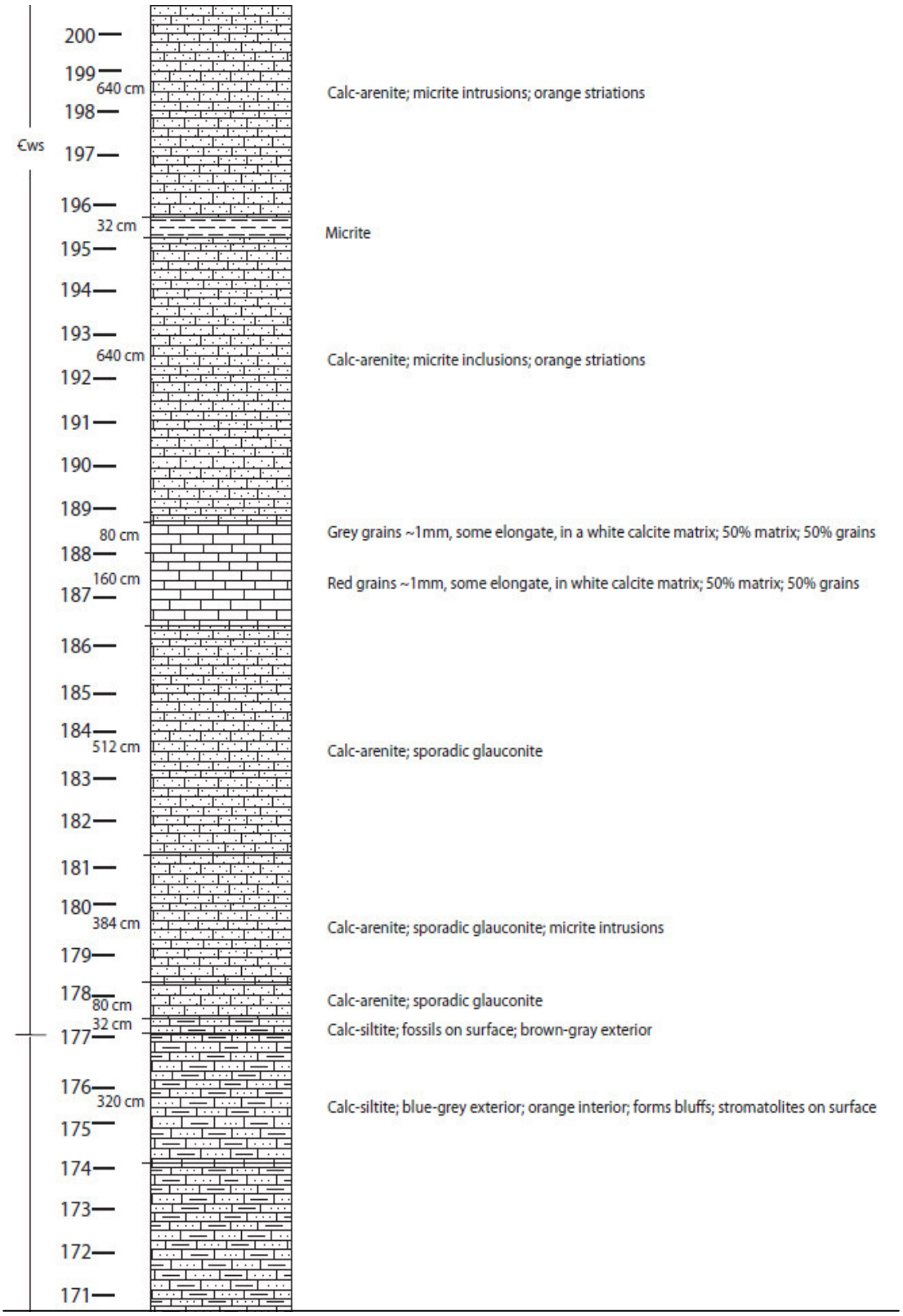
200
199
640 cm
198
197
196
32 cm
195
194
193
640 cm
192
191
190
189
80 cm
188
160 cm
187
186
185
184
512 cm
183
182
181
180
384 cm
179
178
80 cm
32 cm
177
176
320 cm
175
174
173
172
171
Ews
Calc-arenite; micrite intrusions; orange striations
Micrite
Calc-arenite; micrite inclusions; orange striations
Grey grains ~1mm, some elongate, in a white calcite matrix; 50% matrix; 50% grains
Red grains ~1mm, some elongate, in white calcite matrix; 50% matrix; 50% grains
Calc-arenite; sporadic glauconite
Calc-arenite; sporadic glauconite; micrite intrusions
Calc-arenite; sporadic glauconite
Calc-siltite; fossils on surface; brown-gray exterior
Calc-siltite; blue-grey exterior; orange interior; forms bluffs; stromatolites on surface

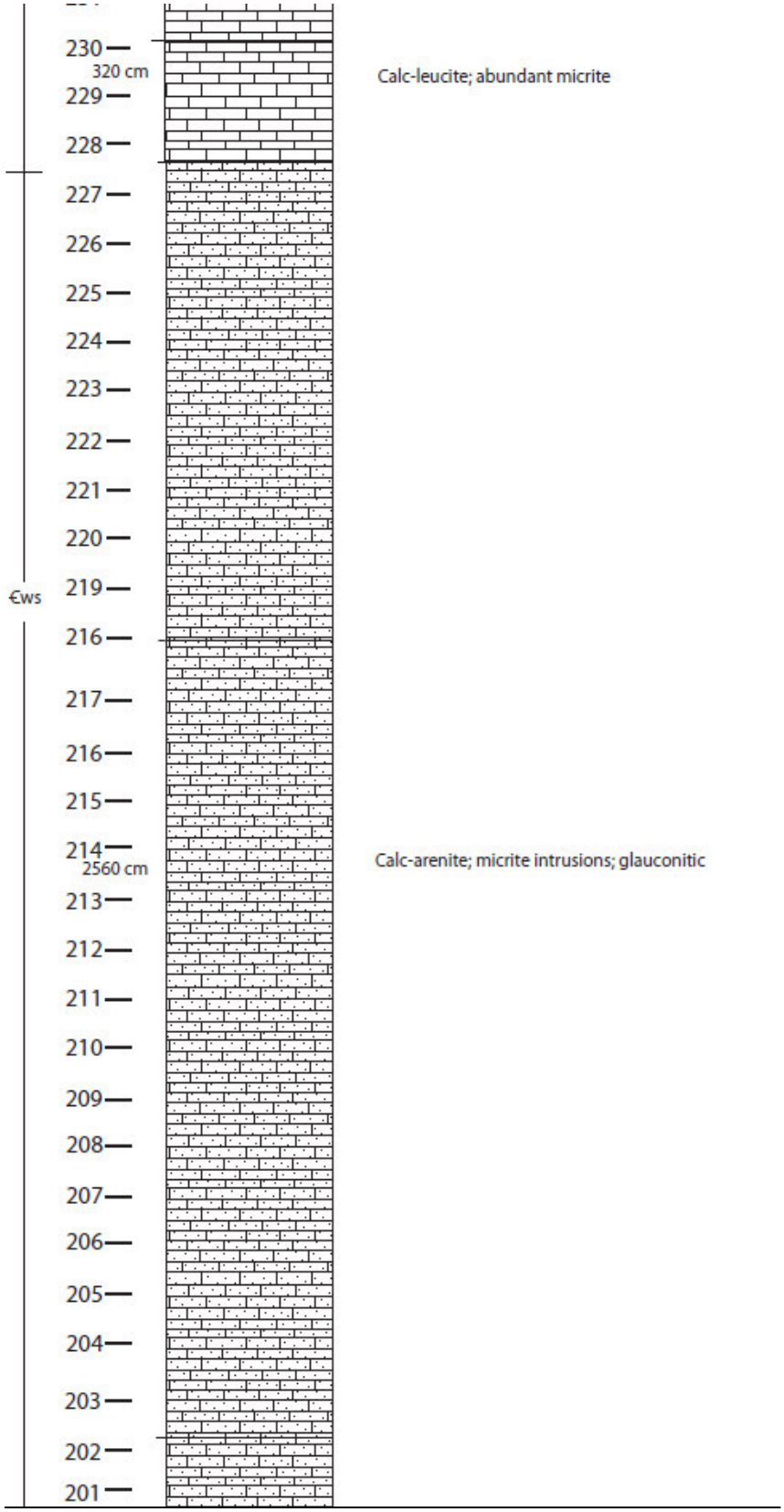
230
320 cm
229
228
227
226
225
224
223
222
221
220
219
€ws
216
217
216
215
214
2560 cm
213
212
211
210
209
208
207
206
205
204
203
202
201
Calc-leucite; abundant micrite
Calc-arenite; micrite intrusions; glauconitic

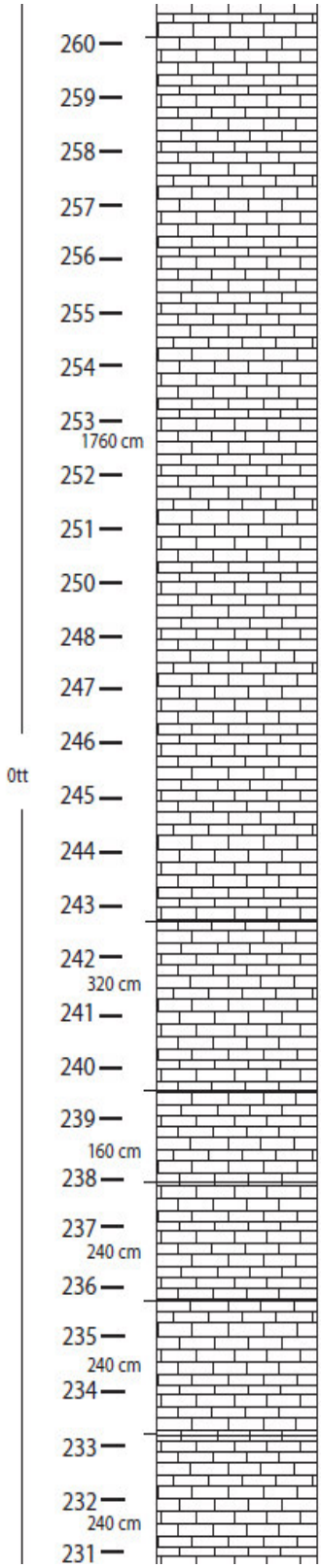

Looks very much like Point Peak limestone; calc-leucite; stromatolites on surface; forms ledges

Less calcite matrix; increasing micrite; orange, grainy inclusions

Large micrite inclusions in calcite matrix; orange, grainy inclusions

Micrite inclusions in calcite matrix; fewer orange inclusions

Less calcite matrix; increasing micrite; orange, grainy inclusions

Large micrite inclusions in calcite matrix; orange, grainy inclusions

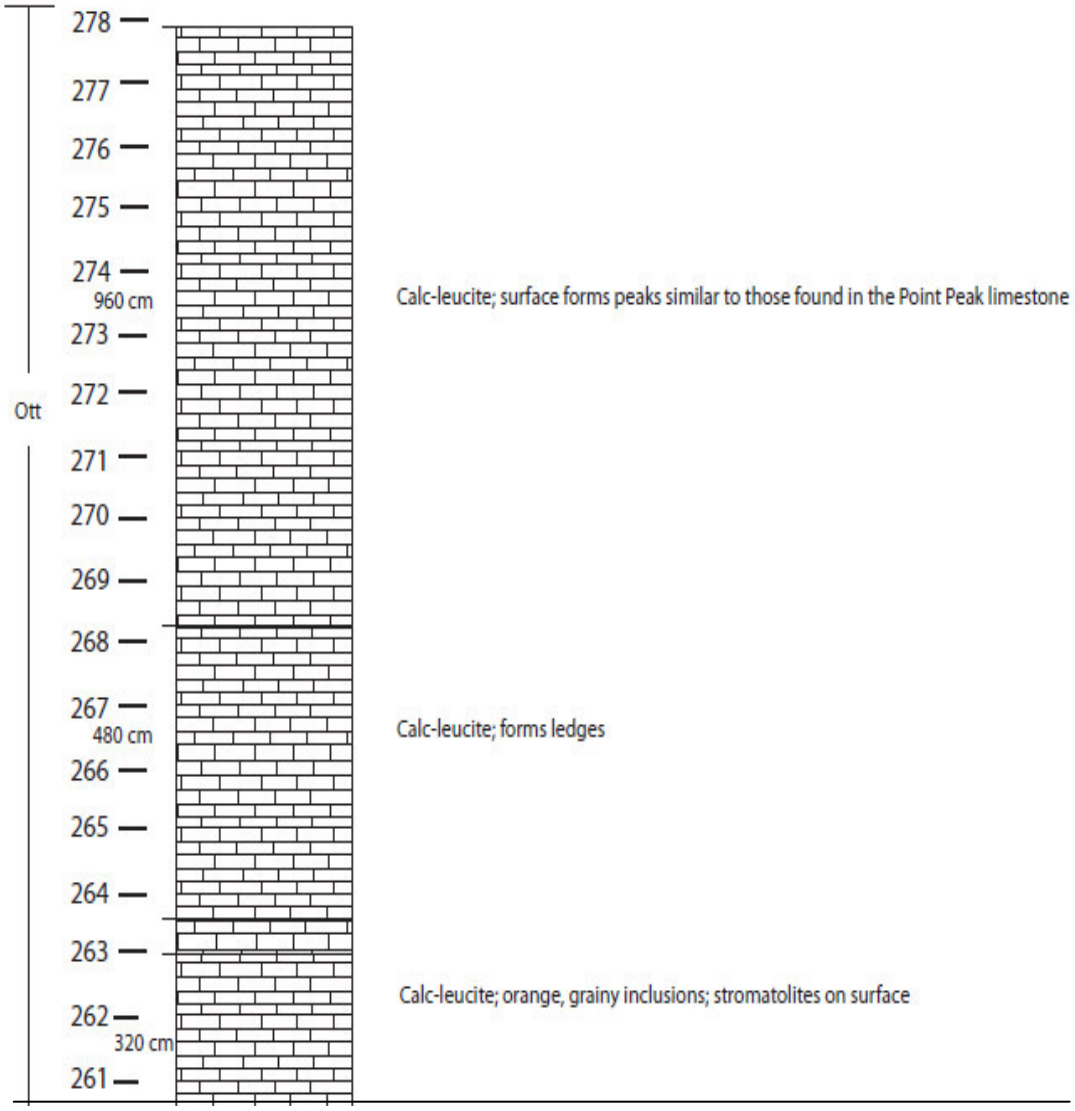
278
277
276
275
274
960 cm
273
272
Ott
271
270
269
268
267
480 cm
266
265
264
263
262
320 cm
261
Calc-leucite; surface forms peaks similar to those found in the Point Peak limestone
Calc-leucite; forms ledges
Calc-leucite; orange, grainy inclusions; stromatolites on surface

VITA

Name: Rebecca Anne Harper
Address: M.S. 3115
Texas A&M University
College Station, Texas 77843-3115

Email Address:raharper11@gmail.com

Education: B.S., Interdisciplinary Studies, Texas A&M University, College Station, 2007

M.S. Geology, Texas A&M University, College Station, 2011